

## **Distal gene regulation mediated by non-coding RNAs contributes to germline risk for breast and prostate cancer**

Nolan Cole<sup>1</sup>, Paige Lee<sup>2</sup>, Tommer Schwarz<sup>3,4</sup>, Pan Zhang<sup>5</sup>, Matthew L. Freedman<sup>6,7</sup>, Alexander Gusev<sup>6</sup>, Sara Lindström<sup>10,11</sup>, Michael J. Gandal<sup>5,12,13</sup>, Bogdan Pasaniuc<sup>4,12,13</sup>, Arjun Bhattacharya<sup>4,14\*</sup>

1. Department of Statistics, Brigham Young University, Provo, UT, United States
2. Department of Statistics, University of California, Los Angeles, CA, United States
3. Bioinformatics Interdepartmental Program, University of California, Los Angeles, CA, United States
4. Department of Pathology and Laboratory Medicine, David Geffen School of Medicine, University of California, Los Angeles, CA, United States
5. Department of Psychiatry, Semel Institute, David Geffen School of Medicine, University of California, Los Angeles, CA, USA
6. Department of Medical Oncology, The Center for Functional Cancer Epigenetics, Dana Farber Cancer Institute, Boston, MA, USA
7. The Center for Cancer Genome Discovery, Dana Farber Cancer Institute, Boston, MA, USA
8. Program in Neurobehavioral Genetics, Semel Institute, David Geffen School of Medicine, University of California, Los Angeles, CA, USA
9. Department of Human Genetics, David Geffen School of Medicine, University of California, Los Angeles, CA, USA
10. Department of Epidemiology, School of Public Health, University of Washington, Seattle, WA, USA
11. Public Health Sciences Division, Fred Hutchinson Cancer Research Center, Seattle, WA, USA
12. Department of Human Genetics, David Geffen School of Medicine, University of California, Los Angeles, CA, USA
13. Department of Computational Medicine, David Geffen School of Medicine, University of California, Los Angeles, CA, USA
14. Institute of Quantitative and Computational Biosciences, David Geffen School of Medicine, University of California, Los Angeles, CA, USA

\*Corresponding author: Arjun Bhattacharya ([abtbhatt@ucla.edu](mailto:abtbhatt@ucla.edu))

## 1 **ABSTRACT**

2 Genome-wide association studies (GWAS) have identified numerous genetic loci associated  
3 with breast and prostate cancer risk, suggesting that germline genetic dysregulation influences  
4 tumorigenesis. However, the biological function underlying many genetic associations is not  
5 well-understood. Previous efforts to annotate loci focused on protein-coding genes (pcGenes)  
6 largely ignore non-coding RNAs (ncRNAs) which account for most transcriptional output in  
7 human cells and can regulate transcription of both pcGenes and other ncRNAs. Though the  
8 biological roles of most ncRNAs are not well-defined, many ncRNAs are involved in cancer  
9 development. Here, we explore one regulatory hypothesis: ncRNAs as *trans*-acting mediators of  
10 gene expression regulation in non-cancerous and tumor breast and prostate tissue. Using  
11 germline genetics as a causal anchor, we categorize distal (>1 Megabase) expression  
12 quantitative trait loci (eQTLs) of pcGenes significantly mediated by local-eQTLs of ncRNAs  
13 (within 1 Megabase). We find over 300 mediating ncRNAs and show the linked pcGenes are  
14 enriched for immunoregulatory and cellular organization pathways. By integrating eQTL and  
15 cancer GWAS results through colocalization and genetically-regulated expression analyses, we  
16 detect overlapping signals in nine known breast cancer loci and one known prostate cancer  
17 locus, and multiple novel genetic associations. Our results suggest a strong transcriptional  
18 impact of ncRNAs in breast and prostate tissue with implications for cancer etiology. More  
19 broadly, our framework can be systematically applied to functional genomic features to  
20 characterize genetic variants distally regulating transcription through *trans*-mechanisms.

21

## 22 **SIGNIFICANCE**

23 This study identifies non-coding RNAs that potentially regulate gene expression in *trans*-  
24 pathways and overlap with genetic signals for breast and prostate cancer susceptibility, with  
25 implications for interpretation of cancer genome-wide association studies.

26

## 27 INTRODUCTION

28 Genome-wide association studies (GWAS) of cancer risk have revealed risk-associated alleles  
29 at hundreds of genetic loci, with breast and prostate cancer GWAS yielding the largest number  
30 of associations (1,2). Through integration with transcriptomic and functional genomics datasets,  
31 the proposed target genes for many of these risk loci have been found in protein-coding regions  
32 of the genome (1–4). However, many risk variants fall in non-coding regions of the genome and,  
33 for these variants, identifying the likely biological mechanism is challenging. One proposed  
34 mechanism for GWAS-identified risk variants is *trans*-acting pathways: a GWAS variant affects  
35 a regulatory feature, like a transcription factor, in proximity, which then affects genes located far  
36 away from the GWAS variant. Particularly, one study identified GWAS risk variants for breast  
37 cancer that confer *trans*-effects through transcription factors, like *ESR1*, *MYC*, and *KLF4* (5).  
38 Another potential mechanism by which GWAS variants in non-coding regions affect risk is  
39 mediation of *trans*-acting effects of genetic variants through non-coding RNAs (ncRNAs).

40  
41 Although ncRNAs do not code for proteins, they account for nearly 60% of transcriptional output  
42 in human cells and interact with a complex network of genes, transcripts, and proteins with  
43 widespread effects on cell biology (6,7). Some ncRNAs, like microRNAs (miRNAs), target and  
44 degrade mRNA transcripts of specific genes and link to regulatory networks that include multiple  
45 ncRNAs and protein-coding genes (pcGenes). These complex interactions between ncRNAs  
46 and pcGenes support the hypothesis that ncRNAs have key roles in cellular pathways (6,8,9).  
47 Specific ncRNAs have been shown to leave their transcription site and regulate gene  
48 expression at genomic regions far from their transcription start site (8,9). However, regulatory  
49 impacts of ncRNAs on transcription of pcGenes are generally uncategorized, especially in a  
50 systematic fashion (8).

51

52 ncRNAs have shown associations with the onset and progression of different cancers, are  
53 enriched in multiple tumor types, and are even therapeutic targets, as they act as regulators of  
54 genes in important tumorigenic or progressive networks (10). For example, the long ncRNA  
55 *XIST* exerts oncogenic and metastatic effects in multiple cancer types (11). Profiling and deep  
56 sequencing of ncRNAs have shown that perturbing ncRNA biogenesis affects amplification,  
57 deletion, and normal epigenetic and transcriptional regulation (10,12–14); accordingly, ncRNAs  
58 can act as oncogenes or antagonize tumor suppressors.

59  
60 However, as most ncRNA mechanisms in cancer tumorigenesis or progression have been  
61 categorized on a case-by-case basis (13,14), mechanistic impacts of ncRNAs have not been  
62 explored systematically. Bioinformatics analyses that leverage high-throughput genomics have  
63 investigated the role of ncRNAs through computational target prediction or differential  
64 expression analyses. Although these computational methods have elucidated potential roles of  
65 ncRNAs in cancer, they have limitations, including computational feasibility and functional  
66 translation of sequence similarity methods (15) and reverse causality for differential expression  
67 analyses (i.e., differential expression more likely reflects consequences of disease) (16).

68  
69 One systematic approach to identifying potential *trans*-mechanisms of regulation is to use  
70 genetic variants as causal anchors. A prevailing thought is that distal expression quantitative  
71 trait loci (eQTLs) of genes, where the genetic variant is far away from the gene (more than 1  
72 Megabase, or Mb), are often themselves local-, or *cis*-acting, QTLs of a regulatory feature (17–  
73 22). We emphasize that the modifiers “local” and “distal” refer merely to distances in the  
74 genome (i.e., within or outside 1 Mb, respectively), whereas *cis*- and *trans*-acting refer to the  
75 biological mechanism (i.e., direct or indirect interaction, respectively). Molecular features, like  
76 ncRNAs, that have potential *trans*-acting regulatory effects can be identified through mediation  
77 analyses, either at variant- or gene-level (18,21,23,24). Not only can these analyses point to

78 distal relationships between ncRNAs and pcGenes, but they can point to genetic variants  
79 associated with disease etiology with potential distal effects in the transcriptome.  
80  
81 Here, we systematically map distal-eQTLs of pcGenes that are potentially mediated by local-  
82 eQTLs of ncRNAs in non-cancerous and tumor prostate and breast tissue, using data from the  
83 Genotype Tissue-Expression (GTEx) Project (25) and The Cancer Genome Atlas (TCGA) (26).  
84 We then employ colocalization (27) and genetically-regulated expression analysis (28) to  
85 identify overlaps in eQTLs and GWAS signals for both overall and molecular subtype-specific  
86 breast (2) and overall prostate (1) cancer risk. In total, our work shows the widespread  
87 transcriptomic impact of genetically-mediated portion of ncRNAs and that this impact has key  
88 associations with cancer susceptibility. This approach provides a rigorous framework to not only  
89 categorize functional hypotheses of distal regulatory effects of ncRNAs but also other regulatory  
90 molecular features.

91

## 92 **MATERIALS AND METHODS**

93 A graphical representation of our methods is provided in **Supplemental Figure S1**.

94

### 95 ***Data acquisition and processing***

96 We used pre-processed genotype, transcriptomic, and covariate data for non-cancerous  
97 mammary and prostate tissue from the Genotype-Tissue Expression Project (GTEx) v8 (25) and  
98 breast and prostate tumor tissue from The Cancer Genome Atlas (TCGA) (26). We included  
99 only individuals of European ancestry due to the small sample sizes available for other  
100 demographics ( $N = 337$  for GTEx breast,  $N = 186$  for GTEx prostate,  $N = 437$  for TCGA  
101 breast,  $N = 349$  for TCGA prostate). For both GTEx and TCGA, we only consider SNPs and  
102 genes on autosomes, restricted to SNPs with minor allele frequency greater than or equal to  
103 1%, and excluded SNPs that deviated from Hardy-Weinberg equilibrium at  $P < 10^{-6}$ .

104

105 We used the BioConductor package *biomaRt* for ENSEMBL gene biotype annotations (29).  
106 Using these annotations, we defined pcGenes as those labeled “protein-coding” and non-coding  
107 RNAs (ncRNAs) as those labeled otherwise; we exclude transcripts labelled as “pseudogenes”.  
108 These annotations included 16,582 pcGenes and 5,650 ncRNAs in GTEx breast, 16,827  
109 pcGenes and 5,862 ncRNAs in GTEx prostate, 21,648 pcGenes and 1,261 ncRNAs in TCGA  
110 breast, and 15,773 pcGenes and 548 ncRNAs in TCGA prostate. We considered all provided  
111 GTEx covariates: 5 genotype-based principal components (PCs), up to 60 probabilistically-  
112 estimated expression residuals (PEER) factors, age, sex, and sequencing platform and protocol  
113 (25). For TCGA, we calculated genotype PCs using PLINK v1.93 (30), calculated up to 50  
114 hidden components of expression (HCP) using *Rhcpp* (31,32), and included the following  
115 covariates: age, estrogen receptor subtype, menopausal status, and disease pathological stage.  
116 For prostate tumors, we include the following covariates: age, sequencing platform, and  
117 protocol.

118

119 We integrated eQTL results with GWAS summary statistics for overall and subtype-specific  
120 breast and overall prostate cancer risk. We obtained European-ancestry specific overall and  
121 subtype-specific GWAS summary statistics for breast cancer risk from the BCAC Consortium  
122 (2). We studied 5 intrinsic breast cancer molecular subtypes, defined by combinations of  
123 estrogen (ER)-, progesterone (PR)-, and human epidermal growth factor receptor (HER2) and  
124 tumor grade (2): Luminal A-like (ER + and/or PR + , HER2-, grade 1 or 2); (2) luminal B-  
125 like/HER2-negative (ER + and/or PR + , HER2-, grade 3); (3) luminal B-like/HER2-positive  
126 (ER + and/or PR + , HER2 +); (4) HER2-positive/non-luminal (ER- and PR-, HER2+), and (5)  
127 TNBC (ER-, PR-, HER2-). We obtained European-ancestry specific GWAS summary statistics  
128 for prostate cancer risk from the PRACTICAL Consortium (1).

129

130 **eQTL mapping**

131 We used a multiple linear regression model in *MatrixEQTL* to detect local- and distal-eQTLs  
132 (33). Here, we define a local-eQTL as a variant within 1 Mb of the gene body and a distal-eQTL  
133 as a variant outside the 1 Mb window. eQTLs outside this 1 Mb window are unlikely to have  
134 direct effects on the promoters or enhancers of the gene and are more likely to have *trans*-  
135 acting mechanisms (17,18).

136  
137 To determine a set of covariates that maximizes the number of detected distal-eQTLs for  
138 pcGenes, we iterated on eQTL mapping using SNPs on Chromosome 22. For breast tumor  
139 tissue, we found that the optimized covariate set for local-eQTL mapping included all of the  
140 clinical covariates (age, estrogen receptor subtype, menopause status, and disease  
141 pathological stage), the first 3 PCs, and the first 8 HCPs. For prostate tumor tissue, we included  
142 age, sequencing platform, protocol as covariates and used 5 genotype PCs and 10 HCPs as the  
143 optimized set of covariates (31). For data from GTEx, we used the full set of provided covariates  
144 for non-cancerous breast and prostate tissue local- and distal-eQTL mapping. We then run  
145 genome-wide eQTL mapping with these optimized sets of covariates.

146

147 **Mediation analysis for distal-eQTL mapping**

148 We first identify a testing triplet, consisting of (1) a SNP  $s$ , (2) a distal pcGene  $G$  associated with  
149 SNP  $s$  with nominal  $P < 10^{-6}$ , and (3) a set of local ncRNAs  $m_1, \dots, m_M$ , all associated with SNP  
150  $s$  with nominal  $P < 10^{-6}$ . As in previous distal-eQTL studies, we use a liberal P-value threshold  
151 to increase the number of testing triplets subjected to rigorous permutation-based mediation  
152 analysis (18,21,23). Next, we fit the following two sets of linear regressions for mediation  
153 analysis (21,23):

154 
$$Y_G = X_s \beta_s + M \beta_M + X_C \beta_C + \epsilon_G, \quad \epsilon_G \sim N(0, \sigma^2 I_n)$$

155 where  $Y_G$  is a vector of expression for gene  $G$ ,  $X_s$  is a vector of dosages for SNP  $s$ ,  $\beta_s$  is the  
156 effect size of SNP  $s$  on gene  $G$ ,  $M$  is the expression matrix of  $m$  ncRNAs,  $\beta_M$  is the effects of the  
157  $M$  ncRNAs on  $Y_G$ ,  $X_C$  is a matrix of covariates, and  $\epsilon_G$  is a random error term. The  $j$ th ncRNA is  
158 modeled as

$$159 \quad M_j = X_s \alpha_{M_j} + X_C \alpha_{C,j} + \epsilon_{M_j}, 1 \leq j \leq m, \quad \epsilon_{M_j} \sim N(0, \sigma_{M_j}^2 I_n)$$

160 where  $M_j$  is the vector of expression for the  $j$ th ncRNA,  $\alpha_{M_j}$  is a vector of effects of SNP  $s$  on  
161 mediator  $M_j$ ,  $X_C$  is a matrix of covariates,  $\alpha_{C,j}$  is a vector of covariate effects on the mediator,  
162 and  $\epsilon_{M_j}$  represents a random error term.

163  
164 We define the total mediation effect (TME) as  $TME = \alpha_M \cdot \beta_M$  and the mediation proportion (MP)  
165 as  $MP = \min(1, \frac{\alpha_M \cdot \beta_M}{\beta_s + \alpha_M \cdot \beta_M})$ . We test  $H_0: TME = 0$  vs.  $H_1: TME \neq 0$  via permutation testing with  
166 10,000 draws.

167  
168 ***Gene-based association testing (GBAT)***

169 We applied GBAT (24) with modifications to identify ncRNAs with genetically-regulated  
170 expression (GReX) associated with distal pcGenes. First, we removed multi-mapped reads  
171 using previously provided annotations (34). Then, we estimated the heritability of ncRNA  
172 expression using GCTA v1.93 (35), excluding genes with limited evidence of heritability ( $P >$   
173  $0.05$ ). Next, using leave-one-out cross-validation, we constructed the ncRNA GReX using SNPs  
174 within 1 Mb using elastic net, LASSO (36) and SuSiE (37), excluding ncRNAs with cross-  
175 validation  $R^2 < 0.01$ . We then employed MatrixEQTL to estimate the association between the  
176 ncRNA GReX and distal pcGene expression, adjusting for the optimized set of covariates from  
177 eQTL mapping (33). Lastly, to identify a set of SNPs that best explains distal ncRNA-pcGene  
178 association, we used SuSiE fine-mapping with default parameters to define a 90% credible set  
179 (37).



180

### 181 ***Colocalization with cancer risk***

182 To identify any potentially overlapping signals between local-eQTLs of ncRNAs, ncRNA-  
183 mediated distal-eQTLs of pcGenes, and cancer risk, we employed the Bayesian colocalization  
184 method, *coloc* (27). *coloc* estimates the posterior probability that the same SNP explains both  
185 the eQTL and the GWAS signal at a given locus. We used standard parameters with default  
186 priors ( $p_1 = 10^{-4}$ ,  $p_2 = 10^{-4}$ , and  $p_{12} = 10^{-6}$ ) to estimate the colocalization posterior probability. We  
187 considered an eQTL signal to colocalize with a GWAS signal if the posterior probability of  
188 colocalization through one SNP (PP.H4 in Giambartolomei et al) was greater than 0.75 (27).

189

### 190 ***Genetically-regulated expression analysis of ncRNAs***

191 We identified any cancer associations for the genetically-regulated expression (GReX) of any  
192 ncRNAs that showed significant mediation of multiple distal-eQTLs of distant pcGenes. First,  
193 using elastic net regression, linear mixed modeling, and SuSiE, we built predictive models of  
194 ncRNAs in both GTEx and TCGA data across breast and prostate tissue and select only models  
195 with 5-fold cross-validation McNemar's adjusted  $R^2 > 0.01$  (28,36–38). We then employed the  
196 weighted burden test and permutation test from the FUSION TWAS framework to detect a trait  
197 association with the GReX of an ncRNA (28). We define transcriptome-wide significance as  $P <$   
198  $2.5 \times 10^{-6}$  and permutation test  $P < 0.05$ .

199

### 200 **Data Availability**

201 GTEx v8 data were obtained through dbGAP Study Accession phs000424.v8.p2. TCGA  
202 genotype were obtained through dbGAP Study Accession phs000178.v11.p8 and expression  
203 and covariate data was obtained from the Broad GDAC Firehose repository  
204 (<https://gdac.broadinstitute.org>). Prostate cancer GWAS summary statistics were obtained from  
205 the Prostate Cancer Association Group to Investigate Cancer Associated Alterations in the

206 Genome (PRACTICAL) Consortium: [http://practical.icr.ac.uk/blog/wp-](http://practical.icr.ac.uk/blog/wp-content/uploads/uploadedfiles/oncoarray/MetaSummaryData/meta_v3_onco_euro_overall_ChromosomesAll_1_release.zip)  
207 [content/uploads/uploadedfiles/oncoarray/MetaSummaryData/meta\\_v3\\_onco\\_euro\\_overall\\_Chromosomes](http://practical.icr.ac.uk/blog/wp-content/uploads/uploadedfiles/oncoarray/MetaSummaryData/meta_v3_onco_euro_overall_ChromosomesAll_1_release.zip)  
208 [All\\_1\\_release.zip](http://practical.icr.ac.uk/blog/wp-content/uploads/uploadedfiles/oncoarray/MetaSummaryData/meta_v3_onco_euro_overall_ChromosomesAll_1_release.zip). Breast cancer GWAS summary statistics were obtained from the Breast  
209 Cancer Association Consortium (BCAC):  
210 [https://bcac.ccge.medschl.cam.ac.uk/bcacdata/oncoarray/oncoarray-and-combined-summary-](https://bcac.ccge.medschl.cam.ac.uk/bcacdata/oncoarray/oncoarray-and-combined-summary-result/gwas-summary-associations-breast-cancer-risk-2020/)  
211 [result/gwas-summary-associations-breast-cancer-risk-2020/](https://bcac.ccge.medschl.cam.ac.uk/bcacdata/oncoarray/oncoarray-and-combined-summary-result/gwas-summary-associations-breast-cancer-risk-2020/). Sample code for this analysis is  
212 available at <https://github.com/CoetheStatistician/ncRNAInBreastCancer/>.

213

## 214 **RESULTS**

215 In this work, we uncover hidden mechanisms contributing to genetic risk for breast and prostate  
216 cancer mediated by ncRNAs, systematically exploring one regulatory hypothesis: distal  
217 mediation of pcGene expression regulation in non-cancerous and tumor breast and prostate  
218 tissue (**Figure 1**). Specifically, we identify distal-eQTLs of protein-coding genes (pcGenes) that  
219 are significantly mediated by ncRNAs local to these distal-eQTLs and assess if they overlap  
220 with genetic signal for cancer risk.

221

### 222 **Multiple ncRNAs mediate distal-eQTLs in breast and prostate tissue**

#### 223 *Distal-eQTL mapping through mediation analysis*

224 We conducted distal-eQTL mapping through ncRNA mediation in GTEx (25) and TCGA (26).  
225 The number of distal-eQTLs of pcGenes that are significantly mediated by ncRNAs are reported  
226 in **Table 1** and **Supplemental Table S1-2**. Distributions of TME and MP in tumor tissue showed  
227 a larger range than in non-cancerous tissue for both breast and prostate, and median TME and  
228 MP were higher in tumor tissue (**Supplemental Figure S2**).

229

230 In non-cancerous breast tissue, pcGenes with cross-chromosomal distal-eQTLs with large  
231 ncRNA-mediated effects included *PUM1* and *PCBP1* (**Figure 2A**), both of which influence

232 tumorigenesis (39–41). In breast tumors, we found *MT4* and *GPRC6A* have large mediated  
233 distal effects. *MT4* belongs to the metallothionein family involved in breast cancer  
234 carcinogenesis (42,43), and *GPRC6A* is a part of the androgen receptor signaling pathway  
235 (44,45). In non-cancerous prostate tissue, we detected large distal mediation effects for genes  
236 such as *RAF1*, a proto-oncogene (46) and *LGR5*, a gene associated with prostatic regeneration  
237 and overexpressed in prostate tumors (47). We also detected a number of olfactory receptors  
238 (*OR2T1*, *OR10G8*, *OR10S1*) with large mediated effects in prostate tumor. Olfactory receptors  
239 are associated with prostate cancer progression but generally have low expression in prostate  
240 tumors (48,49).

241  
242 Owing mainly to a larger set of nominally-significant distal-eQTLs in tumor tissues and larger  
243 sample sizes in TCGA than GTEx, we found nearly four times as many significantly mediated  
244 distal-eQTLs in tumor tissue compared to non-cancerous tissue. Among distal-eQTLs detected  
245 in tumor samples, we observed that multiple ncRNAs mediated distal-eQTLs with many different  
246 pcGenes (vertical bands in **Figure 2A**). One such ncRNA in breast tumors is *LINC00301*,  
247 showing significant mediation of 1,103 distal-eQTLs across 53 unique SNPs and 53 unique  
248 pcGenes. Many of these pcGenes belong to the GAGE protein family, which promotes breast  
249 cancer cell invasion and has shown evidence of distal genetic regulation (50,51). *LINC00301*  
250 itself has been implicated in facilitating tumor progression and immune suppression, albeit in  
251 lung cancer (52). Another example of such an ncRNA in breast tumors is *miR-548f-4*, a  
252 commonly mutated microRNA in multiple cancers (53), mediating more than 300 distal-eQTLs  
253 for 16 unique pcGenes, including *GUCA2B*, upregulated in breast cancer metastases (54), and  
254 *CYP2C9*, a target of tamoxifen (55). In contrast, only two ncRNAs in non-cancerous breast  
255 tissue showed significant mediation of more than 50 distal pcGenes. One of these genes,  
256 *FAM106A*, mediated distal-eQTLs of 13 pcGenes, including *BTN3A2*, a prognostic marker for  
257 breast cancer (56). In both non-cancerous and tumor breast tissue, three pcGenes (*PRCC1*,

258 *CYP2C9*, and *ATG14*) showed significant mediation through ncRNAs, though the sets of  
259 pcGene targets across non-cancerous and tumor tissue are distinct.

260  
261 In prostate tumors, *LINC02903* showed significant mediation with the most distal-eQTLs (177  
262 eQTLs across 8 pcGenes). These pcGenes include *FABP9*, an upregulated gene in prostate  
263 carcinomas with prognostic value (57), and *MTNR1B*, a gene harboring nominal risk variants for  
264 prostate cancer (58). Another ncRNA with significant TME for nearly 100 distal-eQTLs across  
265 20 pcGenes was *SDHAP2*. Many of these pcGenes have been implicated in prostate cancer  
266 and metastasis pathways, including *TMEM207*, *FADS6*, *MTNR1B*, *SLC26A8*, and *FGF23* (59–  
267 61). Similar to breast tissue, only two ncRNAs showed significant mediation of more than 20  
268 distal eQTLs in prostate tissue: *FBXO30-DT* and *SNHG2*, which has been implicated in  
269 tumorigenesis and proliferation in multiple cancers (62–64). A majority (22/26) of distal-eQTLs  
270 mediated by *FBXO30-DT* are for *OVCH2*, which has been implicated in prostate risk through  
271 GWAS (65,66). The majority of distal-eQTLs mediated by *SNHG2* are for *RAF1*, a therapeutic  
272 target for multiple cancers (46). We did not detect any shared ncRNAs or pcGenes across non-  
273 cancerous and tumor prostate tissue.

274  
275 *Gene-based distal-eQTL mapping*

276 Next, we conducted gene-level distal eQTL mapping using GBAT (24) to identify ncRNAs that  
277 are regulated by multiple weak local genetic effects and may have distal effects on pcGenes;  
278 these ncRNAs are likely to be missed by the mediation framework. Comparing to mediated  
279 pcGenes from mediation analysis (**Table 1**), we found a similar order of magnitude of pcGenes  
280 with distal associations with ncRNAs using GBAT (**Table 2**). We again detected far more distal  
281 ncRNA-pcGene directional associations in tumor compared to non-cancerous tissue (**Table 2**,  
282 **Supplemental Table S1-2**). In addition, the distribution of ncRNA-pcGene effect sizes is shifted  
283 downwards in tumor tissue, compared to non-cancerous tissue, though the number of effect

284 sizes in these distributions are far less for non-cancerous tissue distal associations  
285 (**Supplemental Figure S2**). In breast tumors, we found large distal genetic associations with  
286 pcGenes like *OXNAD1*, an RNA-binding protein that is associated with pan-cancer survival  
287 rates and involved with tumor invasion and metastasis (66,67), and *LCN9*, part of the lipocalin  
288 family that promotes breast cancer metastasis (68). In prostate tumors, we detected multiple  
289 large distal genetic associations with genes in the pro-proliferative keratin-associated protein  
290 family (*KRTAP13-3*, *KRTAP13-4*, *KRTAP10-8*) (69) (**Figure 2**).

291  
292 Though distal genetic effects of ncRNAs in non-cancerous breast or prostate tissue were  
293 sparse, we found three ncRNAs with genetic associations with pcGenes across both breast and  
294 prostate tissue: *LINC01678*, *FAM106A*, and *AP001056.1*. These ncRNAs also target the same  
295 pcGenes (*LOC102724159*, *CCDC144A*, *GATD3B*, and a paralog to *TRAPPC10*), all with no  
296 catalogued functions in cancer.

297  
298 Again, in tumor-specific gene-gene associations, many ncRNAs had associations with multiple  
299 pcGenes, leading to vertical bands in the location plots in **Figure 2B**. For example, in breast  
300 tumors, *LINC000906*, a predicted miRNA sponge in breast tumors (70), was associated with  
301 115 pcGenes. The largest association was with *MS4A5*, whose hypomethylation is shown to be  
302 prognostic for multiple cancer types (71,72). Another ncRNA associated with multiple different  
303 pcGenes is *LINC00115*, a known promoter of breast cancer metastasis and progression (73–  
304 75). Many of these targets are related to interferons (*IFNA17* and *IFNW1*), immune system  
305 cytotoxicity (*RAC2* and *DDB2*), or secretory proteins (*PRH1* and *PRH2*).

306  
307 In prostate tumors, *FAM138F* showed distal genetic associations with 57 distinct pcGenes,  
308 many of which are involved in amino acid activation in prostate cancer (*HDAC2*, *NT5DC1*,  
309 *NUS1*, and *PREP*) and protein stability (*PDCD2*, *TCP1*). Additionally *TDRG1*, shown to be

310 associated with progression and metastases in multiple cancers (76,77), showed multiple distal  
311 genetic associations with pcGenes, including the cancer-initiating pluripotency factor *PRDM14*  
312 (78) and multiple genes related to olfactory stimulus (*OR10H3*, *OR2T1*, *OR51V1*, and *UGT2A1*)  
313 (49). Taken together, these distal eQTL mappings suggest the ncRNAs have strong influences  
314 on gene expression of multiple pcGenes in both non-cancerous and tumor tissue.

315

### 316 *Overlap of miRNA-pcGene pairs with target prediction databases*

317 For in-silico validation, we queried TargetScan (79,80), a database that curates computationally  
318 predicted RNA targets of miRNAs, for any miRNAs that our analysis detected to mediate distal-  
319 eQTLs of pcGenes. Out of 522 pairs of miRNAs and pcGenes across 72 unique miRNAs  
320 identified through our analysis, we found that 184 pairs were included in the TargetScan  
321 database (**Supplemental Table S3**). miRNA-pcGene pairs identified in our eQTL analysis are  
322 found in TargetScan at an enrichment ratio of 8.2 (95% CI: [6.68, 10.09]), compared to the  
323 universe of all miRNA-target pairs in TargetScan (approximately 3.56 million) and roughly  
324 159,000 miRNA-target pairs in TargetScan for the 72 miRNA families identified. A majority of  
325 these miRNAs (82% of miRNAs detected in eQTLs) are conserved only across humans and  
326 mice but well-annotated. Though this intersection with TargetScan does not implicate the  
327 miRNA in distal regulation of the proposed pcGene, it provides some computational validation of  
328 this relationship using different methodology (sequence similarity vs. eQTL mapping).

329

### 330 **Distal-eGenes are enriched for tumorigenesis and cancer progression gene pathways**

331 To assess enriched biological processes or pathways by sets of prioritized pcGenes (called  
332 distal-eGenes), we conducted gene ontology enrichments (81). Overall, compared to all  
333 expressed pcGenes in the transcriptome, distal-eGenes in non-cancerous tissue (combining  
334 breast and prostate) were significantly enriched (FDR-adjusted  $P < 0.05$ ) for many relevant  
335 ontologies: immune processes, genes targeted by epigenetic regulation, microRNA targets in

336 cancer, and oxidoreductase activity. In comparison, distal-eGenes detected in tumor tissue  
337 showed enrichments mainly for chemical and sensory receptors and intermediate filament  
338 cytoskeleton (**Supplemental Figure S3-4**). Comparing tissue-prioritized distal-eGenes (breast-  
339 specific or prostate-specific pcGenes to the protein-coding transcriptome), we found distal-  
340 eGenes enrichments detected in prostate tissue for immune pathway ontologies, including the  
341 multiple activations of immune cells, and known tumorigenic pathways, like the JAK-STAT  
342 cascade and PI3K-Akt signaling (82,83). We did not detect any significant enrichments for the  
343 breast-specific distal-eGenes (**Supplemental Figure S5**).

344  
345 We also conducted comparisons of distal-eGenes between non-cancerous and tumor state in  
346 both breast and prostate tissue (**Figure 3**). We find that, compared to distal-eGenes prioritized  
347 in breast tumors, non-cancerous breast distal-eGenes were enriched for cytokine and leukocyte  
348 production, response, and function, as well as membrane transport and binding. We observed  
349 similar enrichments when we compared non-cancerous prostate distal-eGenes to those from  
350 prostate tumors, with additional cell death and morphogenesis ontologies enrichments. In  
351 contrast, across both breast and prostate tissue, tumor-specific distal-eGenes, compared to  
352 non-cancerous distal-eGenes, mainly showed enrichments for olfactory and chemical stimulus  
353 response, intermediate filament cytoskeleton localization, and epidermis development. These  
354 ontologies are consistent with cancer progression, as olfactory receptors have been validated  
355 as prognostic biomarkers in prostate cancers and are overexpressed in more aggressive breast  
356 tumors (48,49,84,85), more aggressive breast cancers are enriched for genes that influence  
357 epidermal growth (86) and cytoskeletal dysregulation is key to cancer cell invasion, progression,  
358 and metastasis (87–89).

359

360 **Distal-eQTLs overlap with genetic signal for breast and prostate cancer risk**



361 Lastly, we integrated these eQTL results with GWAS summary statistics for overall prostate and  
362 overall and molecular subtype-specific breast cancer risk (1,2). A total of 84 detected ncRNAs  
363 are within 0.5 Mb of a GWAS SNP at  $P < 5 \times 10^{-8}$ , the majority for overall prostate and breast  
364 cancer risk, which have the largest GWAS sample sizes (**Figure 4A, Supplemental Table S1-**  
365 **2**). Among pairs of ncRNAs and pcGenes where the ncRNA is 0.5 Mb from a GWAS SNP for  
366 either breast or prostate cancer risk, we identified 30 pairs (15 for overall breast cancer and 10  
367 for LumA breast cancer, five for prostate cancer) where at least one of the ncRNA local-eQTL or  
368 pcGene distal-eQTL colocalized with the GWAS signal at the locus with  $PP.H4 \geq 0.75$   
369 (**Supplemental Figure S6, Supplemental Table S4**). In total, we detected 10 independent  
370 overall or LumA-specific breast cancer risk GWAS signals and one independent prostate cancer  
371 risk GWAS signal may be, in part, explained by distal genetics effects on pcGenes mediated by  
372 local-ncRNAs.

373  
374 We found that distal-eQTLs of *CSH1* mediated by *RFPL1S* strongly colocalize with GWAS  
375 signal for prostate cancer risk. ( $PP.H4 = 0.913$ ) (**Figure 4B**). *CSH1* codes for a somatotropin  
376 hormone with paracrine signaling functions promoting cell division and growth in glands (90).  
377 Using non-cancerous breast tissue eQTLs, we found strong colocalization with overall breast  
378 cancer risk with local-eQTLs of *RUSC1-AS1* and distal-eQTLs of *SH2B1* (**Figure 4C**). Two  
379 different SNPs carried the largest posterior probability of colocalization for the local-  
380 (rs2297480) and distal-eQTLs (rs2075571), which are in moderate, yet statistically significant,  
381 linkage disequilibrium ( $D' = 0.51$ ,  $R^2 = 0.131$ ,  $P < 0.001$ ). *RUSC1-AS1* has shown evidenced  
382 silencing of genes through epigenetic signaling and is correlated with breast cancer progression  
383 (91,92). Additionally, *SH2B1* is involved with cytokine signaling in cell proliferation and migration  
384 (93). We also found strong colocalization with LumA-specific breast cancer risk with local-  
385 eQTLs of *THBS3-AS1* and distal-eQTLs of *SLC39A13* in non-cancerous breast tissue. The  
386 same SNP showed the maximum posterior probability for colocalization with both the local- and



387 distal-eQTL signal. Though the ncRNA has not been implicated in cancer risk or progression,  
388 *SLC39A13* facilitates metastasis in ovarian cancer by activating the Src/FAK signaling pathway  
389 (94).

390  
391 For overall breast cancer risk, we also detect strong colocalization between eQTLs and GWAS  
392 signals at the 17q21.31 locus. This locus houses a large, common inversion polymorphism  
393 associated with breast and ovarian cancer prognosis (95–97), as well as widespread  
394 associations with multiple phenotypes (98–101). In particular, we found that the ncRNA  
395 *KANSL1-AS1* potentially mediates distal-eQTLs of multiple pcGenes. All but one of these  
396 pcGenes are on Chromosome 17, near the end of the 17q21.31 region; the last pcGene we  
397 detected is *TXNRD3* at 3q21.3. We were interested in disentangling effects of the H2 inversion  
398 on gene expression and breast cancer risk, with the proposed causal diagram presented in  
399 **Figure 5A**. First, we estimated haplotypes of the H2 inversion in GTEx (102). We found that  
400 *KANSL1-AS1* and the associated pcGenes near 17q21.31 all have significant associations with  
401 the H2 inversion (**Figure 5B**). Next, we reran mediation analysis for SNPs local to *KANSL-AS1*  
402 and these detected pcGenes. After accounting for H2, the distal mediation signal of *KANSL-AS1*  
403 is attenuated for all pcGenes except *TXNRD3*, suggesting that the inversion may be driving a  
404 significant portion of this signal. These analyses support our proposed causal model, that the  
405 genetics of the H2 inversion affect expression of the local ncRNA *KANSL-AS1* and the distal  
406 pcGenes at the end of the inversion, which induces the eQTL associations (**Figure 5A**).

407  
408 H2 inversion-adjusted colocalization analyses also support this model. A salient example is  
409 shown in **Figure 5D**, with Manhattan plots from colocalization analysis of overall breast cancer  
410 risk, local-eQTLs of *KANSL-AS1*, and distal-eQTLs of *CRHR1*. Colocalization analysis  
411 unadjusted for H2, showed nearly-perfect colocalization for both eQTL signals with GWAS  
412 (PP.H4 > 0.98 for both eQTLs), but after adjustments, the eQTL signals are completely

413 removed. In fact, the standardized effect sizes for local-eQTLs of *KANSL1-AS1* showed strong  
414 correlation with the standardized effect sizes for local-QTLs of the H2 inversion (**Figure 5E**),  
415 and the local-QTL signal for the H2 inversion strongly colocalized (PP.H4 = 0.99) with the  
416 GWAS signal in the locus (**Figure 5F**). These results illustrate that the structural inversion in the  
417 locus likely accounts for both *cis*-genetic control of *KANSL1-AS1* and the associated pcGenes  
418 further downstream on Chromosome 17. Furthermore, we emphasize further examination of the  
419 H2 inversion and other structural variants in the locus for its impact on local and distal gene  
420 expression, as well as cancer susceptibility, especially to elucidate if SNPs with widespread  
421 local or distal associations with gene expression are affected by confounding due to structural  
422 variants or other aberrations.

423

424 We also studied the cancer risk associations of ncRNAs with predicted large transcriptomic  
425 effects using a genetically-regulated expression (GReX) approach (**Methods**). At  $P < 2.5 \times 10^{-6}$   
426 and permutation  $P < 0.05$ , we identify 33 ncRNA-level associations (**Figure 6, Supplemental**  
427 **Table S5**), predominantly for overall and subtype-specific breast cancer risk. Only one ncRNA,  
428 *SDHAP2*, showed an association with overall prostate cancer risk (**Figure 6**); as we restrict to  
429 ncRNAs mediating distal-eQTLs and not necessarily in known prostate cancer GWAS loci, we  
430 do not recover any ncRNAs detected by Guo et al's analysis of long-ncRNAs in prostate cancer  
431 (103). A couple ncRNAs prioritized in associations of breast cancer risk using ncRNA GReX in  
432 non-cancerous breast tissues have been previously noted. Common non-synonymous SNPs in  
433 *HCG9* have previously been implicated in breast cancer GWAS (104). In addition, *CEROX1*, a  
434 cataloged post-transcriptional regulator of mitochondrial catalytic activity, has been implicated in  
435 distal alterations of metabolic pathways in breast cancers (14,105). ncRNAs prioritized in breast  
436 tumor GReX-associations with breast cancer risk mainly included micro- and snoRNAs. Of  
437 these, *miR-519d* has been shown to suppress breast cancer cell growth by targeting distal

438 molecular features(106,107). GReX associations prioritize these ncRNAs for further  
439 investigation of their functional effects in breast and prostate tissue.

440

## 441 **DISCUSSION**

442 In this work, we systematically identify distal-eQTLs of pcGenes that are mediated by ncRNAs  
443 in non-cancerous and tumor breast and prostate tissue. We then show that many of these  
444 ncRNA-mediated distal-eQTLs of pcGenes overlap with GWAS signals for breast and prostate  
445 cancer, both with known GWAS loci and novel genetic loci undetected by GWAS. Taken  
446 together, our results suggest that distal genetic effects on pcGenes mediated by ncRNAs may  
447 be a common mechanism underlying genetic signals and ncRNAs have a widespread role as  
448 distal transcriptional regulators in prostate and breast tissue. We observed more distal ncRNA-  
449 pcGene directional associations in tumor than non-cancerous tissue, suggesting that tumor  
450 tissues have multiple activated gene regulatory networks with potential effects on disease  
451 pathogenesis or progression. Our results implicating distal interactions between ncRNAs and  
452 pcGenes are attractive for further in silico and experimental study.

453

454 We find many colocalized eQTL signals for ncRNAs and pcGenes in the 17q21.31 region, many  
455 of which have been prioritized by previous genetic association studies. For example, a  
456 transcriptome-wide association study (TWAS) of estrogen receptor subtype-specific breast  
457 cancer, identified ncRNA *KANSL-AS1* (108), which has also been associated with ovarian  
458 cancer (109). In our analysis, *KANSL-AS1* mediated multiple breast cancer-associated pcGenes  
459 further downstream on Chromosome 17 and colocalized almost perfectly with the GWAS  
460 association, suggesting widespread distal effects of *KANSL-AS1* (108,110–114). However, after  
461 accounting for the large and common H2 inversion in the 17q21.31 locus, the distal effects of  
462 *KANSL1-AS1* were largely attenuated, pointing to correlated effects of large structural  
463 aberrations on gene expression and disease etiology in this region (115–118). These results

464 also suggest that structural aberrations, like the 17q21.31 H2 inversion, have large effects on  
465 gene expression, not only locally, but also distally. Our results also serve as a cautionary tale:  
466 future gene expression analyses must delineate the eQTL signal in a locus from chromosomal  
467 aberrations, especially when integrating with GWAS signals. Comprehensive analyses of the  
468 transcriptomic effects of genomic aberrations in tumor tissue are needed.

469  
470 We conclude with limitations of our study. First, we rely on Ensembl annotations of gene  
471 biotypes to define our sets of ncRNAs and pcGenes. These annotations may be incomplete,  
472 and accordingly, we may have ignored multiple non-coding transcripts (119). Next, as our local-  
473 and distal-eQTL signals are the same cohort, we were unable to use multi-trait colocalization  
474 methods, like *moloc* or *Primo* (120,121). A more flexible framework that allows for shared  
475 molecular QTL signal could be developed to fully interrogate the mediated-distal QTL signal, in  
476 the context of complex trait etiology. Next, we do not account for copy number variation or  
477 structural variation to disentangle these potentially disparate signals. Future studies should  
478 consider corrections for inversions, translocations, or genomic imbalances. Lastly, due to limited  
479 sample sizes in TCGA, we could not assess the effects of molecular subtype heterogeneity on  
480 eQTL mapping in tumor tissue. Previously, subtype-specific genetic architecture of gene  
481 expression regulation has been suggested by previous studies (5,122,123), with some distal  
482 genetic associations detected for genes that are highly predictive of molecular subtypes (124).  
483 Robust subtype-specific analyses in breast cancer can be informative for both subtype-specific  
484 risk and outcomes.

485  
486 Our study provides evidence supporting *trans*-acting regulation by ncRNAs as a potential  
487 biological mechanism relevant to breast and prostate cancer etiology. Particularly, our results  
488 emphasize that larger samples of tissue- and tumor-specific transcriptomics datasets need to be

489 collected to study often ignored transcripts and explore more complex regulatory hypotheses to  
490 interpret GWAS risk loci for cancer.

491

## 492 REFERENCES

- 493 1. Schumacher FR, Al Olama AA, Berndt SI, Benlloch S, Ahmed M, Saunders EJ, et al.  
494 Association analyses of more than 140,000 men identify 63 new prostate cancer  
495 susceptibility loci. *Nature Genetics*. Nature Publishing Group; 2018;50:928–36.
- 496 2. Zhang H, Ahearn TU, Lecarpentier J, Barnes D, Beesley J, Qi G, et al. Genome-wide  
497 association study identifies 32 novel breast cancer susceptibility loci from overall and  
498 subtype-specific analyses. *Nature Genetics*. *Nat Genet*; 2020;52:572–81.
- 499 3. Michailidou K, Lindström S, Dennis J, Beesley J, Hui S, Kar S, et al. Association analysis  
500 identifies 65 new breast cancer risk loci. *Nature*. Europe PMC Funders; 2017;551:92–4.
- 501 4. Mancuso N, Gayther S, Gusev A, Zheng W, Penney KL, Kote-Jarai Z, et al. Large-scale  
502 transcriptome-wide association study identifies new prostate cancer risk regions. *Nature*  
503 *Communications* [Internet]. Nature Publishing Group; 2018;9. Available from:  
504 <https://www.ncbi.nlm.nih.gov/pmc/articles/PMC6172280/>
- 505 5. Li Q, Seo JH, Stranger B, McKenna A, Pe'Er I, Laframboise T, et al. A novel eQTL-based  
506 analysis reveals the biology of breast cancer risk loci. *Cell*. NIH Public Access;  
507 2013;152:633–633.
- 508 6. Kopp F, Mendell JT. Functional classification and experimental dissection of long noncoding  
509 RNAs. *Cell*. NIH Public Access; 2018;172:393–393.
- 510 7. Abascal F, Acosta R, Addleman NJ, Adrian J, Afzal V, Aken B, et al. Expanded  
511 encyclopaedias of DNA elements in the human and mouse genomes. *Nature*. *Nature*  
512 *Research*; 2020;583:699–710.

- 513 8. Statello L, Guo CJ, Chen LL, Huarte M. Gene regulation by long non-coding RNAs and its  
514 biological functions. *Nature Reviews Molecular Cell Biology* 2020 22:2. Nature Publishing  
515 Group; 2020;22:96–118.
- 516 9. Vance KW, Ponting CP. Transcriptional regulatory functions of nuclear long noncoding  
517 RNAs. *Trends in Genetics*. Elsevier; 2014;30:348–348.
- 518 10. Anastasiadou E, Jacob LS, Slack FJ. Non-coding RNA networks in cancer. *Nature Reviews*  
519 *Cancer* 2017 18:1. Nature Publishing Group; 2017;18:5–18.
- 520 11. Chen DL, Chen LZ, Lu YX, Zhang DS, Zeng ZL, Pan ZZ, et al. Long noncoding RNA XIST  
521 expedites metastasis and modulates epithelial–mesenchymal transition in colorectal  
522 cancer. *Cell Death & Disease* 2017 8:8. Nature Publishing Group; 2017;8:e3011–e3011.
- 523 12. Slack FJ, Chinnaiyan AM. The Role of Non-coding RNAs in Oncology. *Cell. Cell*;  
524 2019;179:1033–55.
- 525 13. Arun G, Diermeier SD, Spector DL. Therapeutic Targeting of Long Non-Coding RNAs in  
526 Cancer. *Trends in molecular medicine*. NIH Public Access; 2018;24:257–257.
- 527 14. Kamada S, Takeiwa T, Ikeda K, Horie-Inoue K, Inoue S. Long Non-coding RNAs Involved  
528 in Metabolic Alterations in Breast and Prostate Cancers. *Frontiers in Oncology*. Frontiers  
529 Media S.A.; 2020;10:2119–2119.
- 530 15. Peterson SM, Thompson JA, Ufkin ML, Sathyanarayana P, Liaw L, Congdon CB. Common  
531 features of microRNA target prediction tools. *Frontiers in Genetics*. Frontiers Research  
532 Foundation; 2014;5:23–23.
- 533 16. Porcu E, Sadler MC, Lepik K, Auwerx C, Wood AR, Weihs A, et al. Differentially expressed  
534 genes reflect disease-induced rather than disease-causing changes in the transcriptome.  
535 *Nature Communications* 2021 12:1. Nature Publishing Group; 2021;12:1–9.
- 536 17. Pierce BL, Tong L, Chen LS, Rahaman R, Argos M, Jasmine F, et al. Mediation Analysis  
537 Demonstrates That Trans-eQTLs Are Often Explained by Cis-Mediation: A Genome-Wide  
538 Analysis among 1,800 South Asians. *PLoS Genetics*. Public Library of Science; 2014;10.

- 539 18. Pierce BL, Tong L, Argos M, Demanelis K, Jasmine F, Rakibuz-Zaman M, et al. Co-  
540 occurring expression and methylation QTLs allow detection of common causal variants and  
541 shared biological mechanisms. *Nature Communications*. Nature Publishing Group;  
542 2018;9:1–12.
- 543 19. Yang F, Gleason KJ, Wang J, Duan J, He X, Pierce BL, et al. CCmed: cross-condition  
544 mediation analysis for identifying replicable trans-associations mediated by cis-gene  
545 expression. *Bioinformatics*. Oxford Academic; 2021;37:2513–20.
- 546 20. Yang F, Wang J, Pierce BL, Chen LS. Identifying cis-mediators for trans-eQTLs across  
547 many human tissues using genomic mediation analysis. *Genome Research*. Cold Spring  
548 Harbor Laboratory Press; 2017;27:1859–71.
- 549 21. Bhattacharya A, Li Y, Love MI. MOSTWAS: Multi-Omic Strategies for Transcriptome-Wide  
550 Association Studies. Zhu X, editor. *PLoS Genetics*. 2021;17:e1009398–e1009398.
- 551 22. Bhattacharya A, Freedman AN, Avula V, Harris R, Liu W, Pan C, et al. Placental genomics  
552 mediates genetic associations with complex health traits and disease. *Nat Commun*.  
553 Nature Publishing Group; 2022;13:706.
- 554 23. Shan N, Wang Z, Hou L. Identification of trans-eQTLs using mediation analysis with  
555 multiple mediators. *BMC Bioinformatics*. BioMed Central Ltd.; 2019;20.
- 556 24. Liu X, Mefford JA, Dahl A, He Y, Subramaniam M, Battle A, et al. GBAT: a gene-based  
557 association test for robust detection of trans-gene regulation. *Genome Biology*. *Genome*  
558 *Biology*; 2020;21:211–211.
- 559 25. Aguet F, Barbeira AN, Bonazzola R, Brown A, Castel SE, Jo B, et al. The GTEx  
560 Consortium atlas of genetic regulatory effects across human tissues. *Science*. American  
561 Association for the Advancement of Science; 2020;369:1318–30.
- 562 26. Weinstein JN, Collisson EA, Mills GB, Shaw KRM, Ozenberger BA, Ellrott K, et al. The  
563 cancer genome atlas pan-cancer analysis project. *Nature Genetics*. Nature Publishing  
564 Group; 2013;45:1113–20.



- 565 27. Giambartolomei C, Vukcevic D, Schadt EE, Franke L, Hingorani AD, Wallace C, et al.  
566 Bayesian Test for Colocalisation between Pairs of Genetic Association Studies Using  
567 Summary Statistics. Williams SM, editor. PLoS Genetics. Public Library of Science;  
568 2014;10:e1004383–e1004383.
- 569 28. Gusev A, Ko A, Shi H, Bhatia G, Chung W, Penninx BWJH, et al. Integrative approaches  
570 for large-scale transcriptome-wide association studies. Nature Genetics. 2016;48:245–52.
- 571 29. Durinck S, Spellman PT, Birney E, Huber W. Mapping identifiers for the integration of  
572 genomic datasets with the R/Bioconductor package biomaRt. Nature Protocols 2009 4:8.  
573 Nature Publishing Group; 2009;4:1184–91.
- 574 30. Purcell S, Neale B, Todd-Brown K, Thomas L, Ferreira MAR, Bender D, et al. PLINK: A  
575 Tool Set for Whole-Genome Association and Population-Based Linkage Analyses. Am J  
576 Hum Genet. 2007;81:559–75.
- 577 31. Mostafavi S, Battle A, Zhu X, Urban AE, Levinson D, Montgomery SB, et al. Normalizing  
578 RNA-Sequencing Data by Modeling Hidden Covariates with Prior Knowledge. PLoS ONE.  
579 Public Library of Science; 2013;8:e68141–e68141.
- 580 32. van Iterson M. mvaniterson/Rhcpp: A fast R implementation using Rcpp based on the  
581 original matlab HCP method for Normalizing RNA-Sequencing Data by Modeling Hidden  
582 Covariates with Prior Knowledge [Internet]. 2020. Available from:  
583 <https://github.com/mvaniterson/Rhcpp>
- 584 33. Shabalin AA. Gene expression Matrix eQTL: ultra fast eQTL analysis via large matrix  
585 operations. Bioinformatics (Oxford, England). Oxford University Press; 2012;28:1353–8.
- 586 34. Saha A, Battle A. False positives in trans-eQTL and co-expression analyses arising from  
587 RNA-sequencing alignment errors [version 2; peer review: 3 approved]. F1000Research.  
588 F1000 Research Ltd; 2019;7:1860–1860.
- 589 35. Yang J, Lee SH, Goddard ME, Visscher PM. GCTA: a tool for genome-wide complex trait  
590 analysis. American journal of human genetics. Elsevier; 2011;88:76–82.



- 591 36. Friedman J, Hastie T, Tibshirani R. Regularization Paths for Generalized Linear Models via  
592 Coordinate Descent. *Journal of Statistical Software*. 2010;33:1–22.
- 593 37. Wang G, Sarkar A, Carbonetto P, Stephens M. A simple new approach to variable  
594 selection in regression, with application to genetic fine mapping. *Journal of the Royal  
595 Statistical Society: Series B*. Blackwell Publishing Ltd; 2020;82:1273–300.
- 596 38. Endelman JB. Ridge Regression and Other Kernels for Genomic Selection with R Package  
597 rrBLUP. *The Plant Genome*. 2011;4:250–5.
- 598 39. Carrasco AM, Acosta O, Ponce J, Cotrina J, Aguilar A, Araujo J, et al. PUM1 and RNase P  
599 genes as potential cell-free DNA markers in breast cancer. *Journal of Clinical Laboratory  
600 Analysis*. John Wiley & Sons, Ltd; 2021;35:e23720–e23720.
- 601 40. Shi P, Zhang J, Li X, Li W, Li H, Fu P. Long non-coding RNA NORAD inhibition upregulates  
602 microRNA-323a-3p to suppress tumorigenesis and development of breast cancer through  
603 the PUM1/eIF2 axis. <https://doi.org/10.1080/1538410120211934627>. Taylor & Francis;  
604 2021;20:1295–307.
- 605 41. Shi H, Li H, Yuan R, Guan W, Zhang X, Zhang S, et al. PCBP1 depletion promotes  
606 tumorigenesis through attenuation of p27Kip1 mRNA stability and translation. *Journal of  
607 Experimental & Clinical Cancer Research* 2018 37:1. BioMed Central; 2018;37:1–18.
- 608 42. Goulding H, Jasani B, Pereira H, Reid A, Galea M, Bell J, et al. Metallothionein expression  
609 in human breast cancer. *British Journal of Cancer* 1995 72:4. Nature Publishing Group;  
610 1995;72:968–72.
- 611 43. Si M, Lang J. The roles of metallothioneins in carcinogenesis. *Journal of Hematology &  
612 Oncology* 2018 11:1. BioMed Central; 2018;11:1–20.
- 613 44. Michmerhuizen AR, Spratt DE, Pierce LJ, Speers CW. Are we there yet? Understanding  
614 androgen receptor signaling in breast cancer. *npj Breast Cancer* 2020 6:1. Nature  
615 Publishing Group; 2020;6:1–19.

- 616 45. Masi M, Garattini E, Bolis M, Di Marino D, Maraccani L, Morelli E, et al. OXER1 and  
617 RACK1-associated pathway: a promising drug target for breast cancer progression.  
618 *Oncogenesis* 2020 9:12. Nature Publishing Group; 2020;9:1–15.
- 619 46. Zhang L, Pattanayak A, Li W, Ko H-K, Fowler G, Gordon R, et al. A Multifunctional Therapy  
620 Approach for Cancer: Targeting Raf1- Mediated Inhibition of Cell Motility, Growth, and  
621 Interaction with the Microenvironment. *Molecular Cancer Therapeutics*. American  
622 Association for Cancer Research; 2020;19:39–51.
- 623 47. Wang B, Wang X, Long JE, Eastham-Anderson J, Firestein R, Junttila MR. Castration-  
624 Resistant Lgr5+ Cells Are Long-Lived Stem Cells Required for Prostatic Regeneration.  
625 *Stem Cell Reports*. Elsevier; 2015;4:768–768.
- 626 48. Abaffy T, Bain JR, Muehlbauer MJ, Spasojevic I, Lodha S, Bruguera E, et al. A  
627 Testosterone Metabolite 19-Hydroxyandrostenedione Induces Neuroendocrine Trans-  
628 Differentiation of Prostate Cancer Cells via an Ectopic Olfactory Receptor. *Frontiers in*  
629 *Oncology*. Frontiers; 2018;0:162–162.
- 630 49. Neuhaus EM, Zhang W, Gelis L, Deng Y, Noldus J, Hatt H. Activation of an Olfactory  
631 Receptor Inhibits Proliferation of Prostate Cancer Cells. *The Journal of Biological*  
632 *Chemistry*. American Society for Biochemistry and Molecular Biology; 2009;284:16218–  
633 16218.
- 634 50. Maine EA, Westcott JM, Precht AM, Dang TT, Whitehurst AW, Pearson GW. The cancer-  
635 testis antigens SPANX-A/C/D and CTAG2 promote breast cancer invasion. *Oncotarget*.  
636 Impact Journals, LLC; 2016;7:14708–14708.
- 637 51. Quiroz-Zárate A, Harshfield BJ, Hu R, Knoblauch N, Beck AH, Hankinson SE, et al.  
638 Expression Quantitative Trait loci (QTL) in tumor adjacent normal breast tissue and breast  
639 tumor tissue. Wong K-K, editor. *PLOS ONE*. Public Library of Science; 2017;12:e0170181–  
640 e0170181.

- 641 52. Sun C-C, Zhu W, Li S-J, Hu W, Zhang J, Zhuo Y, et al. FOXC1-mediated LINC00301  
642 facilitates tumor progression and triggers an immune-suppressing microenvironment in  
643 non-small cell lung cancer by regulating the HIF1 $\alpha$  pathway. *Genome Medicine* 2020 12:1.  
644 BioMed Central; 2020;12:1–27.
- 645 53. Tuna M, Machado AS, Calin GA. Genetic and epigenetic alterations of microRNAs and  
646 implications for human cancers and other diseases. *Genes Chromosomes and Cancer*.  
647 Blackwell Publishing Inc.; 2016;55:193–214.
- 648 54. Xiao L, Zhou J, Liu H, Zhou Y, Chen W, Cui W, et al. RNA Sequence Profiling Reveals  
649 Unique Immune and Metabolic Features of Breast Cancer Brain Metastases. *Frontiers in*  
650 *Oncology*. *Frontiers*; 2021;0:3213–3213.
- 651 55. MC B, U Y, MO B, O S, A B. Tamoxifen inhibits cytochrome P450 2C9 activity in breast  
652 cancer patients. *Journal of chemotherapy (Florence, Italy)*. *J Chemother*; 2006;18:421–4.
- 653 56. Cai P, Lu Z, Wu J, Qin X, Wang Z, Zhang Z, et al. BTN3A2 serves as a prognostic marker  
654 and favors immune infiltration in triple-negative breast cancer. *Journal of Cellular*  
655 *Biochemistry*. John Wiley & Sons, Ltd; 2020;121:2643–54.
- 656 57. MS AF, X G, SS F, W A-J, Z B, PR R, et al. The increased expression of fatty acid-binding  
657 protein 9 in prostate cancer and its prognostic significance. *Oncotarget*. *Oncotarget*;  
658 2016;7:82783–97.
- 659 58. MJ M, S L, NE A, CA H, D A, A B, et al. Association of type 2 diabetes susceptibility  
660 variants with advanced prostate cancer risk in the Breast and Prostate Cancer Cohort  
661 Consortium. *American journal of epidemiology*. *Am J Epidemiol*; 2012;176:1121–9.
- 662 59. Marín-Aguilera M, Reig Ò, Lozano JJ, Jiménez N, García-Recio S, Erill N, et al. Molecular  
663 profiling of peripheral blood is associated with circulating tumor cells content and poor  
664 survival in metastatic castration-resistant prostate cancer. *Oncotarget*. *Impact Journals*,  
665 LLC; 2015;6:10604–10604.

- 666 60. Saigo C, Kito Y, Takeuchi T. Cancerous Protein Network That Inhibits the Tumor  
667 Suppressor Function of WW Domain-Containing Oxidoreductase (WWOX) by Aberrantly  
668 Expressed Molecules. *Frontiers in Oncology*. Frontiers; 2018;0:350–350.
- 669 61. S F, J W, Y Z, C J C, M I. FGF23 promotes prostate cancer progression. *Oncotarget*.  
670 *Oncotarget*; 2015;6:17291–301.
- 671 62. Li Y-L, Tian H, Jiang J, Zhang Y, Qi X-W. Multifaceted regulation and functions of fatty acid  
672 desaturase 2 in human cancers. *American Journal of Cancer Research*. e-Century  
673 Publishing Corporation; 2020;10:4098–4098.
- 674 63. Chi J-R, Yu Z-H, Liu B-W, Zhang D, Ge J, Yu Y, et al. SNHG5 Promotes Breast Cancer  
675 Proliferation by Sponging the miR-154-5p/PCNA Axis. *Molecular Therapy - Nucleic Acids*.  
676 Elsevier; 2019;17:138–49.
- 677 64. Damas ND, Marcatti M, Côme C, Christensen LL, Nielsen MM, Baumgartner R, et al.  
678 SNHG5 promotes colorectal cancer cell survival by counteracting STAU1-mediated mRNA  
679 destabilization. *Nature Communications* 2016 7:1. Nature Publishing Group; 2016;7:1–14.
- 680 65. Wang M, Takahashi A, Liu F, Ye D, Ding Q, Qin C, et al. Large-scale association analysis  
681 in Asians identifies new susceptibility loci for prostate cancer. *Nature Communications*  
682 2015 6:1. Nature Publishing Group; 2015;6:1–7.
- 683 66. Sinnott-Armstrong N, Seoane JA, Sallari R, Pritchard JK, Curtis C, Snyder MP. Convergent  
684 mutations in tissue-specific regulatory regions reveal novel cancer drivers. *bioRxiv*. Cold  
685 Spring Harbor Laboratory; 2020;2020.08.21.239954-2020.08.21.239954.
- 686 67. Kang D, Lee Y, Lee J-S. RNA-Binding Proteins in Cancer: Functional and Therapeutic  
687 Perspectives. *Cancers*. Multidisciplinary Digital Publishing Institute (MDPI); 2020;12:1–33.
- 688 68. Hu C, Yang K, Li M, Huang W, Zhang F, Wang H. Lipocalin 2: a potential therapeutic target  
689 for breast cancer metastasis. *OncoTargets and therapy*. Dove Press; 2018;11:8099–8099.

- 690 69. Sack LM, Davoli T, Li MZ, Li Y, Xu Q, Naxerova K, et al. Profound Tissue Specificity in  
691 Proliferation Control Underlies Cancer Drivers and Aneuploidy Patterns. *Cell*. NIH Public  
692 Access; 2018;173:499–499.
- 693 70. Zhang J, Xu T, Liu L, Zhang W, Zhao C, Li S, et al. LMSM: A modular approach for  
694 identifying lncRNA related miRNA sponge modules in breast cancer. *PLOS Computational  
695 Biology*. Public Library of Science; 2020;16:e1007851.
- 696 71. Smith JC, Sheltzer JM. Genome-wide identification and analysis of prognostic features in  
697 human cancers. *bioRxiv*. Cold Spring Harbor Laboratory; 2021;2021.06.01.446243-  
698 2021.06.01.446243.
- 699 72. Sun L, Zhang Y, Zhang C. Distinct Expression and Prognostic Value of MS4A in Gastric  
700 Cancer. *Open Medicine*. De Gruyter; 2018;13:178–178.
- 701 73. Hou R, Jiang L. LINC00115 promotes stemness and inhibits apoptosis of ovarian cancer  
702 stem cells by upregulating SOX9 and inhibiting the Wnt/ $\beta$ -catenin pathway through  
703 competitively binding to microRNA-30a. *Cancer Cell International* 2021 21:1. *BioMed  
704 Central*; 2021;21:1–15.
- 705 74. Li Q, Wang X, Zhou L, Jiang M, Zhong G, Xu S, et al. A Positive Feedback Loop of Long  
706 Noncoding RNA LINC00152 and KLF5 Facilitates Breast Cancer Growth. *Frontiers in  
707 Oncology*. *Frontiers*; 2021;0:899–899.
- 708 75. Yuan C, Luo X, Duan S, Guo L. Long noncoding RNA LINC00115 promotes breast cancer  
709 metastasis by inhibiting miR-7. *FEBS Open Bio*. John Wiley & Sons, Ltd; 2020;10:1230–7.
- 710 76. Ma Y, Xu XL, Huang HG, Li YF, Li ZG. LncRNA TDRG1 promotes the aggressiveness of  
711 gastric carcinoma through regulating miR-873-5p/HDGF axis. *Biomedicine &  
712 Pharmacotherapy*. Elsevier Masson; 2020;121:109425–109425.
- 713 77. Hu X, Mu Y, Wang J, Zhao Y. LncRNA TDRG1 promotes the metastasis of NSCLC cell  
714 through regulating miR-873-5p/ZEB1 axis. *Journal of Cellular Biochemistry*. John Wiley &  
715 Sons, Ltd; 2021;122:969–82.

- 716 78. Tracey LJ, Justice MJ. Off to a bad start: Cancer initiation by pluripotency regulator  
717 PRDM14. *Trends in genetics : TIG*. NIH Public Access; 2019;35:489–489.
- 718 79. Agarwal V, Bell GW, Nam J-W, Bartel DP. Predicting effective microRNA target sites in  
719 mammalian mRNAs. Izaurrealde E, editor. *eLife*. eLife Sciences Publications, Ltd;  
720 2015;4:e05005.
- 721 80. McGeary SE, Lin KS, Shi CY, Pham TM, Bisaria N, Kelley GM, et al. The biochemical basis  
722 of microRNA targeting efficacy. *Science*. 2019;366:eaav1741.
- 723 81. Liao Y, Wang J, Jaehnig EJ, Shi Z, Zhang B. WebGestalt 2019: gene set analysis toolkit  
724 with revamped UIs and APIs. *Nucleic Acids Research*. 2019;47:199–205.
- 725 82. Thomas SJ, Snowden JA, Zeidler MP, Danson SJ. The role of JAK/STAT signalling in the  
726 pathogenesis, prognosis and treatment of solid tumours. *British Journal of Cancer* 2015  
727 113:3. Nature Publishing Group; 2015;113:365–71.
- 728 83. Hoxhaj G, Manning BD. The PI3K–AKT network at the interface of oncogenic signalling and  
729 cancer metabolism. *Nature Reviews Cancer* 2019 20:2. Nature Publishing Group;  
730 2019;20:74–88.
- 731 84. Masjedi S, Zwiebel LJ, Giorgio TD. Olfactory receptor gene abundance in invasive breast  
732 carcinoma. *Scientific Reports* 2019 9:1. Nature Publishing Group; 2019;9:1–12.
- 733 85. Kalra S, Mittal A, Gupta K, Singhal V, Gupta A, Mishra T, et al. Analysis of single-cell  
734 transcriptomes links enrichment of olfactory receptors with cancer cell differentiation status  
735 and prognosis. *Communications Biology* 2020 3:1. Nature Publishing Group; 2020;3:1–10.
- 736 86. Feng Y, Spezia M, Huang S, Yuan C, Zeng Z, Zhang L, et al. Breast cancer development  
737 and progression: Risk factors, cancer stem cells, signaling pathways, genomics, and  
738 molecular pathogenesis. *Genes & Diseases*. Chongqing Medical University; 2018;5:77–77.
- 739 87. Holle AW, Kalafat M, Ramos AS, Seufferlein T, Kemkemer R, Spatz JP. Intermediate  
740 filament reorganization dynamically influences cancer cell alignment and migration.  
741 *Scientific Reports* 2017 7:1. Nature Publishing Group; 2017;7:1–14.

- 742 88. Ong MS, Deng S, Halim CE, Cai W, Tan TZ, Huang RYJ, et al. Cytoskeletal Proteins in  
743 Cancer and Intracellular Stress: A Therapeutic Perspective. *Cancers* [Internet].  
744 Multidisciplinary Digital Publishing Institute (MDPI); 2020;12. Available from:  
745 /pmc/articles/PMC7017214/
- 746 89. Tang Y, He Y, Zhang P, Wang J, Fan C, Yang L, et al. LncRNAs regulate the cytoskeleton  
747 and related Rho/ROCK signaling in cancer metastasis. *Molecular Cancer* 2018 17:1.  
748 BioMed Central; 2018;17:1–10.
- 749 90. Strous GJ, Almeida ADS, Putters J, Schantl J, Sedek M, Slotman JA, et al. Growth  
750 Hormone Receptor Regulation in Cancer and Chronic Diseases. *Frontiers in*  
751 *Endocrinology*. Frontiers Media S.A.; 2020;11:867–867.
- 752 91. Hu CC, Liang YW, Hu JL, Liu LF, Liang JW, Wang R. LncRNA RUSC1-AS1 promotes the  
753 proliferation of breast cancer cells by epigenetic silence of KLF2 and CDKN1A. *European*  
754 *review for medical and pharmacological sciences*. *Eur Rev Med Pharmacol Sci*;  
755 2019;23:6602–11.
- 756 92. Zhu L, Cui K, Weng L, Yu P, Du Y, Zhang T, et al. A panel of 8-lncRNA predicts prognosis  
757 of breast cancer patients and migration of breast cancer cells. *PLOS ONE*. Public Library of  
758 Science; 2021;16:e0249174–e0249174.
- 759 93. Yousaf N, Deng Y, Kang Y, Riedel H. Four PSM/SH2-B Alternative Splice Variants and  
760 Their Differential Roles in Mitogenesis \*. *Journal of Biological Chemistry*. Elsevier;  
761 2001;276:40940–8.
- 762 94. Cheng X, Wang J, Liu C, Jiang T, Yang N, Liu D, et al. Zinc transporter SLC39A13/ZIP13  
763 facilitates the metastasis of human ovarian cancer cells via activating Src/FAK signaling  
764 pathway. *Journal of Experimental and Clinical Cancer Research*. BioMed Central Ltd;  
765 2021;40:1–15.



- 766 95. Permut-Wey J, Lawrenson K, Shen HC, Velkova A, Tyrer JP, Chen Z, et al. Identification  
767 and molecular characterization of a new ovarian cancer susceptibility locus at 17q21.31.  
768 Nature communications. NIH Public Access; 2013;4:1627–1627.
- 769 96. Ruiz-Arenas C, Cáceres A, Moreno V, González JR. Common polymorphic inversions at  
770 17q21.31 and 8p23.1 associate with cancer prognosis. Human Genomics. BioMed Central  
771 Ltd.; 2019;13:1–9.
- 772 97. Orsetti B, Courjal F, Cuny M, Rodriguez C, Theillet C. 17q21-q25 aberrations in breast  
773 cancer: combined allelotyping and CGH analysis reveals 5 regions of allelic imbalance  
774 among which two correspond to DNA amplification. Oncogene 1999 18:46. Nature  
775 Publishing Group; 1999;18:6262–70.
- 776 98. O'Brien HE, Hannon E, Hill MJ, Toste CC, Robertson MJ, Morgan JE, et al. Expression  
777 quantitative trait loci in the developing human brain and their enrichment in  
778 neuropsychiatric disorders. Genome Biology [Internet]. BioMed Central; 2018;19. Available  
779 from: [/pmc/articles/PMC6231252/](https://pubmed.ncbi.nlm.nih.gov/30000000/)
- 780 99. Trampush JW, Yang MLZ, Yu J, Knowles E, Davies G, Liewald DC, et al. GWAS meta-  
781 analysis reveals novel loci and genetic correlates for general cognitive function: a report  
782 from the COGENT consortium. Molecular Psychiatry 2017 22:3. Nature Publishing Group;  
783 2017;22:336–45.
- 784 100. Wei XT, Feng GJ, Zhang H, Xu Q, Ni JJ, Zhao M, et al. Pleiotropic genomic variants at  
785 17q21.31 associated with bone mineral density and body fat mass: a bivariate genome-  
786 wide association analysis. European Journal of Human Genetics 2020 29:4. Nature  
787 Publishing Group; 2020;29:553–63.
- 788 101. Bowles KR, Pugh DA, Farrell K, Han N, Tcw J, Liu Y, et al. 17q21.31 sub-haplotypes  
789 underlying H1-associated risk for Parkinson's disease are associated with LRRC37A/2  
790 expression in astrocytes. bioRxiv. Cold Spring Harbor Laboratory; 2021;860668–860668.



- 791 102. Boettger LM, Handsaker RE, Zody MC, Mccarroll SA. Structural haplotypes and recent  
792 evolution of the human 17q21.31 region. *Nature genetics*. NIH Public Access;  
793 2012;44:881–881.
- 794 103. Guo H, Ahmed M, Zhang F, Yao CQ, Li S, Liang Y, et al. Modulation of long noncoding  
795 RNAs by risk SNPs underlying genetic predispositions to prostate cancer. *Nat Genet*.  
796 2016;48:1142–50.
- 797 104. Michailidou K, Hall P, Gonzalez-Neira A, Ghoussaini M, Dennis J, Milne RL, et al. Large-  
798 scale genotyping identifies 41 new loci associated with breast cancer risk. *Nature*  
799 *Genetics*. 2013;45:353–61.
- 800 105. Sirey TM, Roberts K, Haerty W, Bedoya-Reina O, Granados SR, Tan JY, et al. The long  
801 non-coding rna cerox1 is a post transcriptional regulator of mitochondrial complex i  
802 catalytic activity. *eLife*. eLife Sciences Publications Ltd; 2019;8.
- 803 106. Deng X, Zhao Y, Wang B. miR-519d-mediated downregulation of STAT3 suppresses  
804 breast cancer progression. *Oncology reports*. *Oncol Rep*; 2015;34:2188–94.
- 805 107. Li D, Song H, Wu T, Xie D, Hu J, Zhao J, et al. MiR-519d-3p suppresses breast cancer  
806 cell growth and motility via targeting LIM domain kinase 1. *Molecular and cellular*  
807 *biochemistry*. *Mol Cell Biochem*; 2018;444:169–78.
- 808 108. Feng H, Gusev A, Pasaniuc B, Wu L, Long J, Abu-full Z, et al. Transcriptome-wide  
809 association study of breast cancer risk by estrogen-receptor status. *Genetic*  
810 *Epidemiology*. John Wiley & Sons, Ltd; 2020;44:442–68.
- 811 109. Gusev A, Lawrenson K, Lin X, Lyra PC, Kar S, Vavra KC, et al. A transcriptome-wide  
812 association study of high-grade serous epithelial ovarian cancer identifies new  
813 susceptibility genes and splice variants. *Nature Genetics*. Nature Publishing Group;  
814 2019;51:815–23.

- 815 110. Pashirzad M, Fiuji H, Khazei M, Moradi-Binabaj M, Ryzhikov M, Shabani M, et al. Role of  
816 Wnt3a in the pathogenesis of cancer, current status and prospective. *Molecular Biology*  
817 *Reports*. Springer Netherlands; 2019;46:5609–16.
- 818 111. Wu Y, Ginther C, Kim J, Mosher N, Chung S, Slamon D, et al. Expression of Wnt3  
819 activates Wnt/ $\beta$ -catenin pathway and promotes EMT-like phenotype in trastuzumab-  
820 resistant HER2-overexpressing breast cancer cells. *Molecular cancer research : MCR*.  
821 *Mol Cancer Res*; 2012;10:1597–606.
- 822 112. Zhou JX, Yang X, Ning S, Wang L, Wang K, Zhang Y, et al. Identification of KANSARL as  
823 the first cancer predisposition fusion gene specific to the population of European ancestry  
824 origin. *Oncotarget*. Impact Journals, LLC; 2017;8:50594–50594.
- 825 113. Wu W, Li D, Feng X, Zhao F, Li C, Zheng S, et al. A pan-cancer study of selenoprotein  
826 genes as promising targets for cancer therapy. *BMC Medical Genomics*. BioMed Central  
827 Ltd; 2021;14:1–14.
- 828 114. Yu Y, Hu H, Doust AN, Kellogg EA. Divergent gene expression networks underlie  
829 morphological diversity of abscission zones in grasses. *New Phytologist*.  
830 2019;nph.16087-nph.16087.
- 831 115. de Jong S, Chepelev I, Janson E, Strengman E, van den Berg LH, Veldink JH, et al.  
832 Common inversion polymorphism at 17q21.31 affects expression of multiple genes in  
833 tissue-specific manner. *BMC Genomics*. BioMed Central; 2012;13:1–6.
- 834 116. Lu Y, Beeghly-Fadiel A, Wu L, Guo X, Li B, Schildkraut JM, et al. A transcriptome-wide  
835 association study among 97,898 women to identify candidate susceptibility genes for  
836 epithelial ovarian cancer risk. *Cancer Research*. *Cancer Res*; 2018;78:5419–30.
- 837 117. Su X, Li W, Lv L, Li X, Yang J, Luo XJ, et al. Transcriptome-Wide Association Study  
838 Provides Insights Into the Genetic Component of Gene Expression in Anxiety. *Frontiers in*  
839 *Genetics*. Frontiers Media S.A.; 2021;12:1901–1901.

- 840 118. Lee CT, Bendriem RM, Kindberg AA, Worden LT, Williams MP, Drgon T, et al. Functional  
841 Consequences of 17q21.31/WNT3-WNT9B Amplification in hPSCs with Respect to  
842 Neural Differentiation. *Cell Reports*. Cell Press; 2015;10:616–32.
- 843 119. Zhang D, Guelfi S, Garcia-Ruiz S, Costa B, Reynolds RH, D'Sa K, et al. Incomplete  
844 annotation has a disproportionate impact on our understanding of Mendelian and  
845 complex neurogenetic disorders. *Science Advances*. American Association for the  
846 Advancement of Science; 2020;6:8299–8299.
- 847 120. Giambartolomei C, Liu JZ, Zhang W, Hauberg M, Shi H, Boockock J, et al. A Bayesian  
848 framework for multiple trait colocalization from summary association statistics.  
849 *Bioinformatics*. Oxford University Press; 2018;34:2538–45.
- 850 121. Gleason KJ, Yang F, Pierce BL, He X, Chen LS. Primo: Integration of multiple GWAS and  
851 omics QTL summary statistics for elucidation of molecular mechanisms of trait-associated  
852 SNPs and detection of pleiotropy in complex traits. *Genome Biology*. BioMed Central Ltd;  
853 2020;21:236–236.
- 854 122. Bhattacharya A, García-Closas M, Olshan AF, Perou CM, Troester MA, Love MI. A  
855 framework for transcriptome-wide association studies in breast cancer in diverse study  
856 populations. *Genome Biology*. BioMed Central; 2020;21:42–42.
- 857 123. Geeleher P, Nath A, Wang F, Zhang Z, Barbeira AN, Fessler J, et al. Cancer expression  
858 quantitative trait loci (eQTLs) can be determined from heterogeneous tumor gene  
859 expression data by modeling variation in tumor purity. *Genome Biology*. BioMed Central;  
860 2018;19:130–130.
- 861 124. Patel A, Garcia-Closas M, Olshan AF, Perou CM, Troester MA, Love MI, et al. Gene level  
862 germline contributions to clinical risk of recurrence scores in Black and White breast  
863 cancer patients. *Cancer Research*. American Association for Cancer Research;  
864 2021;canres.1207.2021-canres.1207.2021.
- 865

866 **ACKNOWLEDGEMENTS**

867 We thank Nicholas Mancuso, Harold Pimentel, Mike Love, Achal Patel, and Kangcheng Hou for  
868 engaging conversation during the research process. We also thank the UCLA Bruins-in-  
869 Genomics Summer Program for the research opportunities.

870

871 The Prostate cancer genome-wide association analyses are supported by the Canadian  
872 Institutes of Health Research, European Commission's Seventh Framework Programme grant  
873 agreement n° 223175 (HEALTH-F2-2009-223175), Cancer Research UK Grants C5047/A7357,  
874 C1287/A101118, C1287/A16563, C5047/A3354, C5047/A10692, C16913/A6135, and The  
875 National Institute of Health (NIH) Cancer Post-Cancer GWAS initiative grant: No. 1 U19 CA  
876 148537-01 (the GAME-ON initiative).

877

878 Genotyping of the OncoArray was funded by the US National Institutes of Health (NIH) [U19 CA  
879 148537 for ELucidating Loci Involved in Prostate cancer SuscEptibility (ELLIPSE) project and  
880 X01HG007492 to the Center for Inherited Disease Research (CIDR) under contract number  
881 HHSN268201200008I] and by Cancer Research UK grant A8197/A16565. Additional analytic  
882 support was provided by NIH NCI U01 CA188392 (PI: Schumacher).

883

884 We would also like to thank the following for funding support: The Institute of Cancer Research  
885 and The Everyman Campaign, The Prostate Cancer Research Foundation, Prostate Research  
886 Campaign UK (now PCUK), The Orchid Cancer Appeal, Rosetrees Trust, The National Cancer  
887 Research Network UK, The National Cancer Research Institute (NCRI) UK. We are grateful for  
888 support of NIHR funding to the NIHR Biomedical Research Centre at The Institute of Cancer  
889 Research and The Royal Marsden NHS Foundation Trust.

890

891 The breast cancer genome-wide association analyses for BCAC and CIMBA were supported by  
892 Cancer Research UK (C1287/A10118, C1287/A16563, C1287/A10710, C12292/A20861,  
893 C12292/A11174, C1281/A12014, C5047/A8384, C5047/A15007, C5047/A10692,  
894 C8197/A16565), The National Institutes of Health (CA128978, X01HG007492- the DRIVE  
895 consortium), the PERSPECTIVE project supported by the Government of Canada through  
896 Genome Canada and the Canadian Institutes of Health Research (grant GPH-129344) and the  
897 Ministère de l'Économie, Science et Innovation du Québec through Genome Québec and the  
898 PSRSIIRI-701 grant, the Quebec Breast Cancer Foundation, the European Community's  
899 Seventh Framework Programme under grant agreement n° 223175 (HEALTH-F2-2009-223175)  
900 (COGS), the European Union's Horizon 2020 Research and Innovation Programme (634935  
901 and 633784), the Post-Cancer GWAS initiative (U19 CA148537, CA148065 and CA148112 -  
902 the GAME-ON initiative), the Department of Defence (W81XWH-10-1-0341), the Canadian  
903 Institutes of Health Research (CIHR) for the CIHR Team in Familial Risks of Breast Cancer  
904 (CRN-87521), the Komen Foundation for the Cure, the Breast Cancer Research Foundation  
905 and the Ovarian Cancer Research Fund. All studies and funders are listed in Zhang H et al (Nat  
906 Genet, 2020).

907

## 908 **FUNDING**

909 TS was supported by the National Institute of Neurological Disorders and Stroke of the National  
910 Institutes of Health under Award Number T32NS048004. This research was supported by the  
911 National Institute of Mental Health of the National Institutes of Health under Award number  
912 5R01MH115676-04. AG was partially supported by R01 CA227237. SL was partially supported  
913 by NIH award R01 CA194393. BP were partially supported by NIH awards R01 HG009120, R01  
914 MH115676, R01 CA251555, R01 AI153827, R01 HG006399, R01 CA244670, U01 HG011715.  
915 The content is solely the responsibility of the authors and does not necessarily represent the  
916 official views of the National Institutes of Health.

917

918 **AUTHOR INFORMATION**

919 *Contributions*

920 AB conceived the study. AB, TS, and PL developed the statistical approaches, performed the  
921 analysis, and drafted the paper. AB, TS, and BP provided insight in methodological approaches  
922 and analysis. BP provided data resources. AB and BP supervised the study. All authors  
923 approved and edited the final manuscript.

924

925 *Corresponding author*

926 Correspondence to Arjun Bhattacharya (abtbhatt@ucla.edu)

927

928 **ETHICS DECLARATION**

929 *Ethics approval and consent to participate*

930 This study was approved by the Office of Human Research Ethics at the University of California,  
931 Los Angeles, and written informed consent was obtained from each participant. All experimental  
932 methods abided by the Helsinki Declaration.

933

934 *Consent for publication*

935 Not applicable.

936

937 *Competing interests*

938 The authors declare that they have no competing interests.

## FIGURES

Regulation via potential gene activation/inhibition

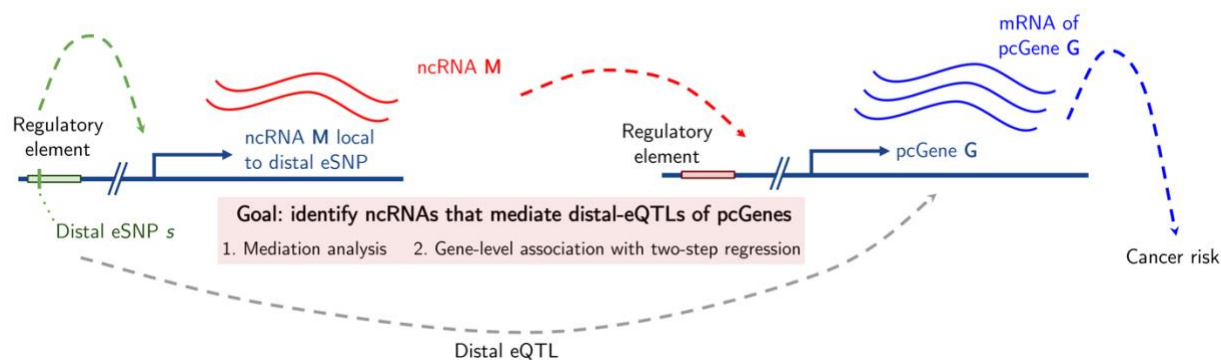


**Figure 1:** Schematic of mediation analysis to identify ncRNA-mediated distal-eQTLs of protein-coding genes. A SNP  $s$  is distal to protein-coding gene  $G$  and local to ncRNA  $M$ , where  $M$  has some distal regulatory effect on  $G$ . We use expression quantitative trait locus mapping to identify the local-eQTL between  $s$  and  $M$  (green dotted line) and the distal-eQTL between  $s$  and  $G$  (grey dotted line). Using either mediation analysis or gene-level association testing, we estimate the indirect mediation effect of  $s$  on  $G$  through effects from  $M$  (red line). Lastly, we use colocalization and genetically-regulated expression analysis to find any intersecting genetic signal between distal-eQTLs of  $G$  and genetic associations with breast and prostate cancer risk.



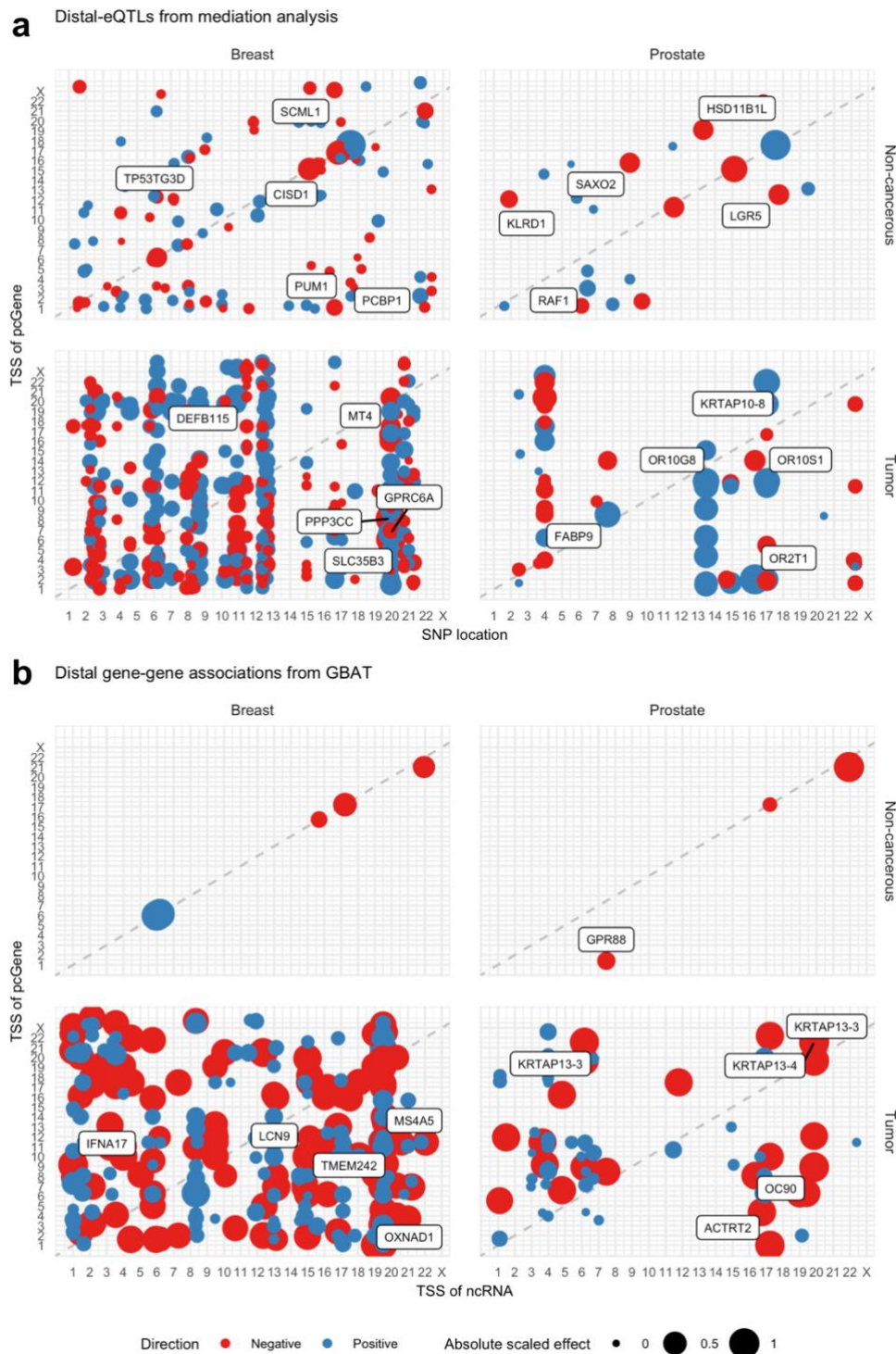


**Figure 2:** Location plot of distal-eQTL or gene-gene associations across healthy and tumor samples of breast and prostate tissue. **(a)** eSNP (X-axis) position vs. transcription start site (TSS) of pcGene (Y-axis) at FDR-adjusted  $P < 0.01$ , sized by absolute scaled TME and colored by direction of effect. **(b)** ncRNA TSS (X-axis) vs. pcGene TSS (Y-axis) at FDR-adjusted  $P < 0.01$ , sized by absolute scaled gene-gene effect and colored by direction of effect. Top cross-chromosomal distal-eGenes with largest effects are labeled.



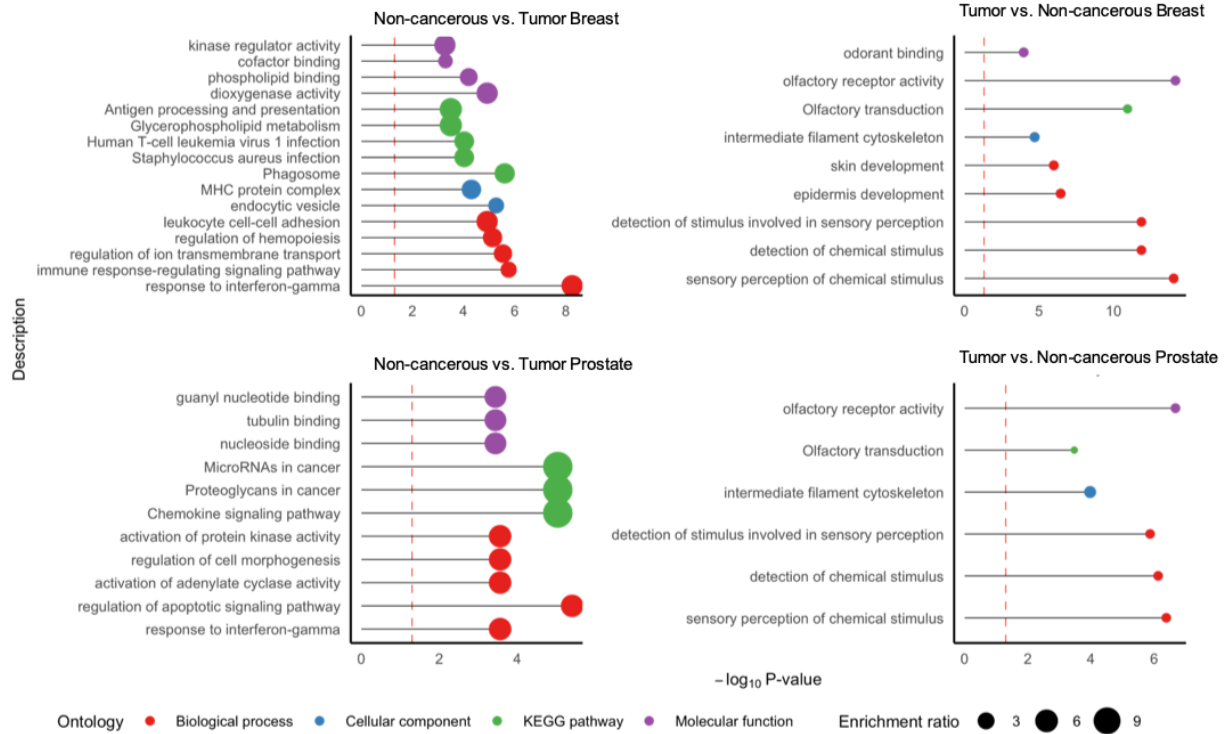


**Figure 3:** Over-represented ontologies for tissue-specific eGenes.  $-\log_{10}$  P-value of enrichment (X-axis) of over-represented gene sets (Y-axis), with point sized by enrichment ratio and colored by ontology category. Here, for a tissue, we compare the set of pcGenes from healthy or tumor state to the universe of all pcGenes for tissue across both healthy and tumor states.

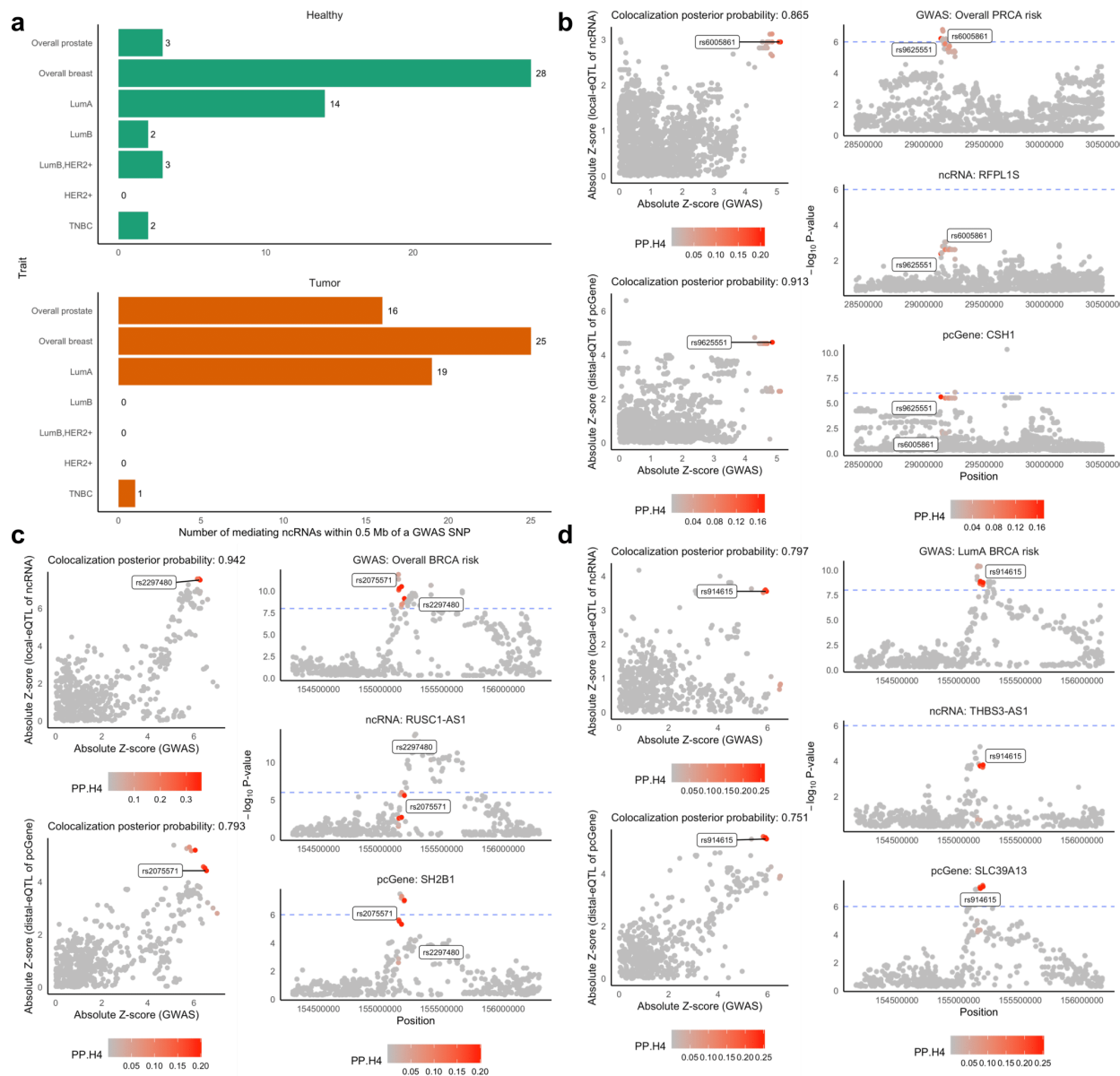


**Figure 4: Colocalization of local-eQTLs of ncRNA and distal-eQTLs of pcGene with GWAS. (a)** Barplot of numbers of mediating ncRNAs within 1 Megabase of a GWAS SNP (X-axis) from cancers (Y-axis). **(b-d)** Colocalization results for example ncRNAs and pcGenes, with phenotype in the GWAS, ncRNA, and pcGene provided. Left panel shows scatterplot of absolute Z-scores of GWAS (X-axis) and eQTL associations (Y-axis) with points colored by posterior probability of colocalization (PP.H4). Right panel shows a Manhattan plot of GWAS (top), ncRNA local-eQTL (middle), and pcGene distal-eQTL (bottom) signal, colored by PP.H4.

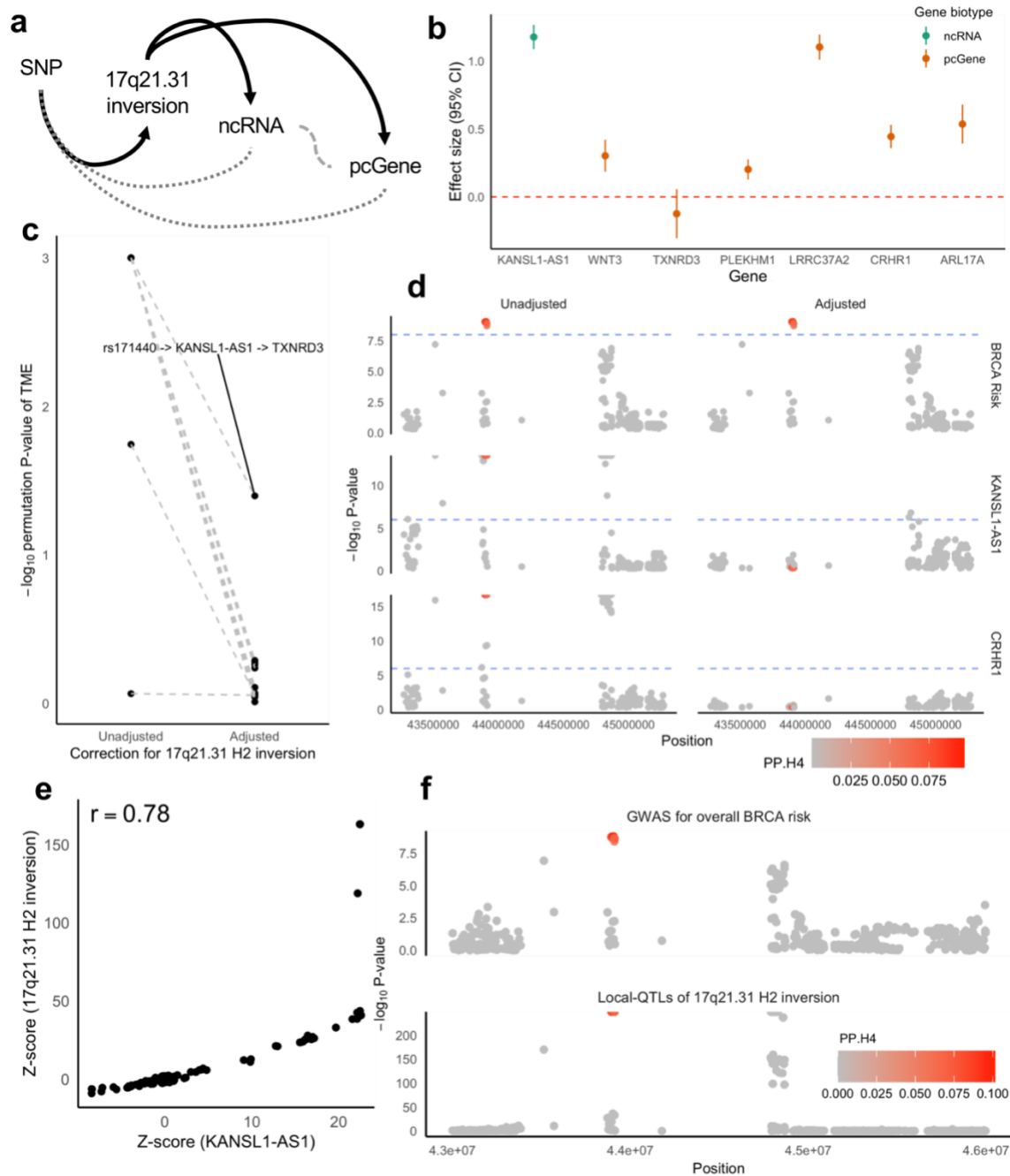


**Figure 5: Impact of H2 inversion on eQTLs in the 17q21.31 locus.** (a) Causal diagram of genetic effects in 17q21.31, where strong effects of genetically-determined H2 inversion on ncRNA and pcGene (in black) induces the observed SNP-ncRNA and -pcGene associations (in grey). (b) Forest plot of effect sizes and 95% confidence interval (Y-axis) on H2 inversion on pcGenes or ncRNAs (X-axis). (c) Difference in  $-\log_{10}$  permutation P-value (Y-axis) of total mediation effect of ncRNA on pcGene, with or without adjustment for H2 inversion (X-axis). (d) Manhattan plots of GWAS, local-eQTLs of KANSL1-AS1, and distal-eQTLs of CRHR1, unadjusted (left) and adjusted (right) for H2 inversion, colored by per-SNP PP.H4. (e) Scatterplot of Z-score of local-eQTLs on KANSL1-AS1 (X-axis) against Z-score of local-QTLs of H2 inversion. (f) Manhattan plots of GWAS and local-QTLs of H2 inversion, colored by per-SNP PP.H4.

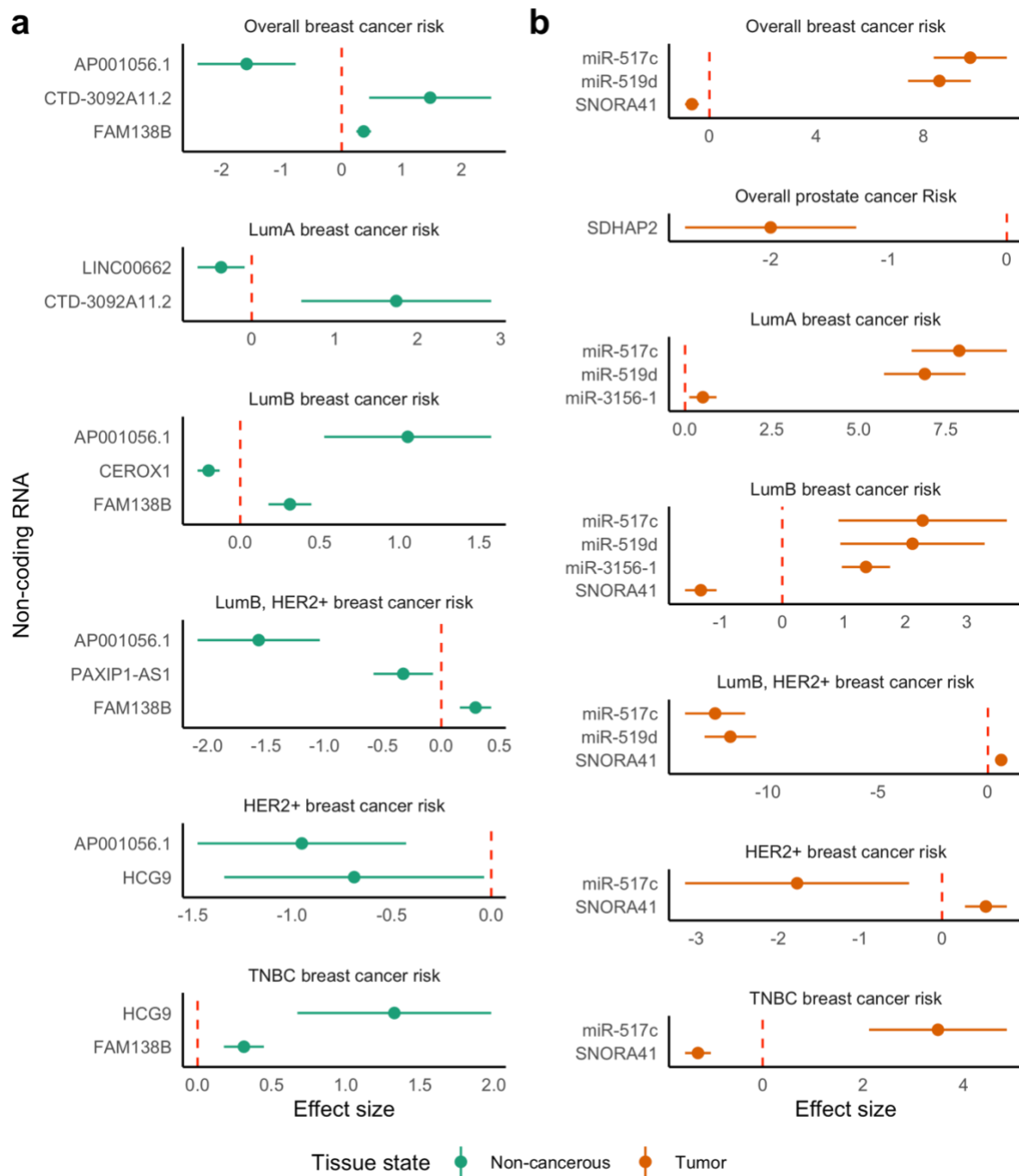


**Figure 6:** GReX associations with cancer risk for ncRNAs mediating multiple distal-eQTLs of pcGenes. Forest plot of effect size and confidence intervals at significance level of  $P = 2.5 \times 10^{-6}$  (Y-axis) of GReX-associations with overall and subtype-specific cancer risk across ncRNAs that showed significant mediation of multiple distal-eQTLs of distinct pcGenes (X-axis) in non-cancerous (a) and tumor (b) tissue states.

## TABLES

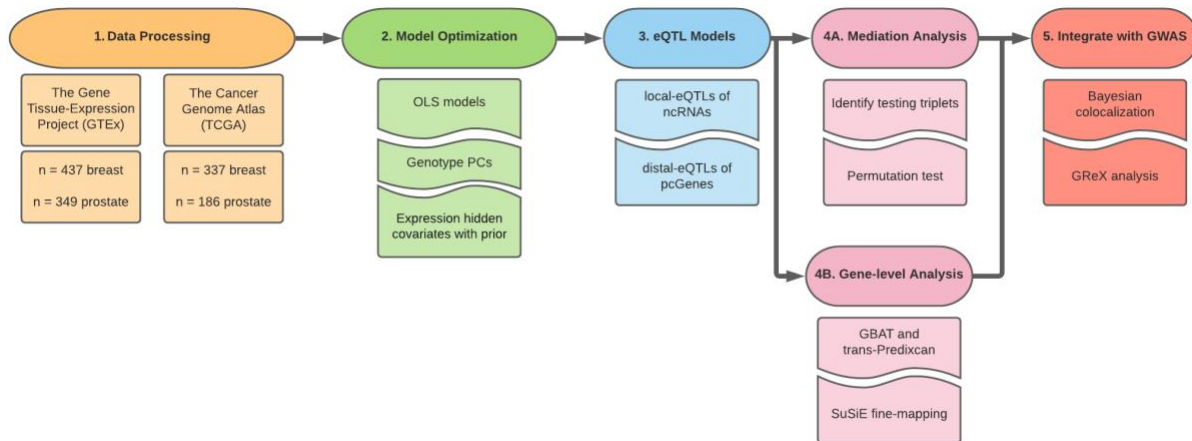
**Table 1:** Summary of local- and distal-eQTL mapping results across breast and prostate non-cancerous and tumor tissue through mediation analysis.

		<i>Breast</i>		<i>Prostate</i>	
		Non-cancerous	Tumor	Non-cancerous	Tumor
<b>Total eQTLs</b>					
	<i>Local</i>	22,832	1,298	12,511	6,368
	<i>Distal</i>	29,512	316,097	31,782	363,587
<b>Total eGenes</b>					
	<i>local-ncRNAs</i>	1,113	87	773	60
	<i>distal-pcGenes</i>	8,849	19,376	8,711	15,560
<b>SNPs associated in both local and distal eQTLs</b>					
	<i>Local</i>	1,569	601	281	6,368
	<i>Distal</i>	1,580	5,089	264	9,259
<b>Mediated distal-eQTLs</b>					
	<i>eSNPs</i>	703	3,017	103	425
	<i>e-ncRNAs</i>	157	45	22	18
	<i>e-pcGenes</i>	173	562	24	107

**Table 2:** Summary of distal-eQTL mapping results across breast and prostate normal and tumor tissue using GBAT.

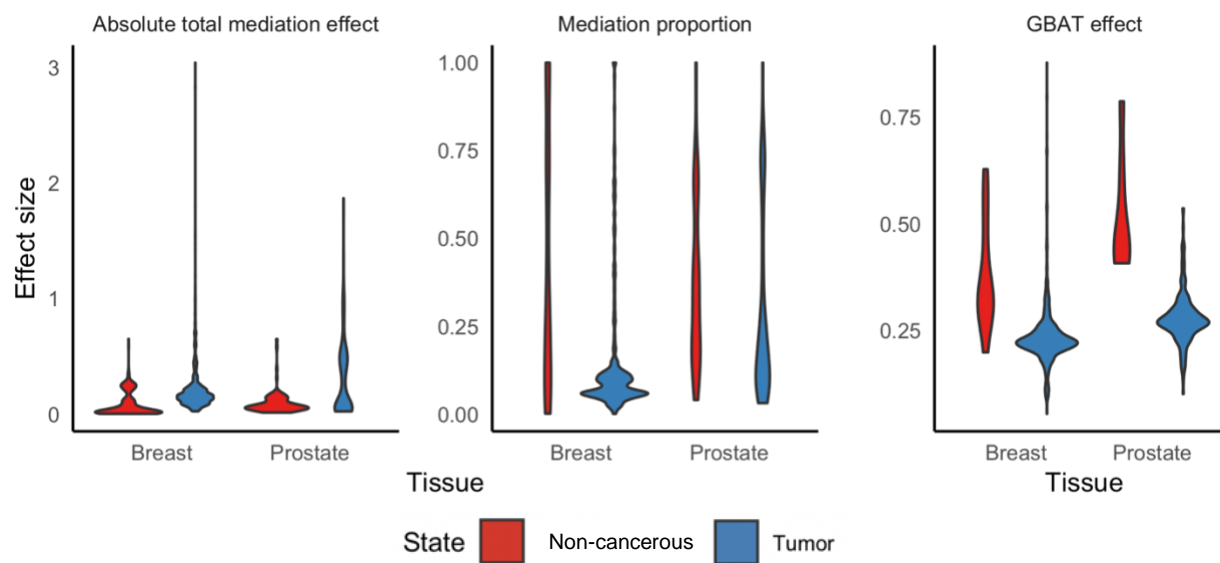
	<i>Breast</i>		<i>Prostate</i>	
	Normal	Tumor	Normal	Tumor
<i>Total gene-gene associations</i>	13	1,375	7	297
<i>Unique ncRNAs</i>	9	209	4	84
<i>Unique pcGenes</i>	10	1,127	5	268

## SUPPLEMENTAL FIGURES

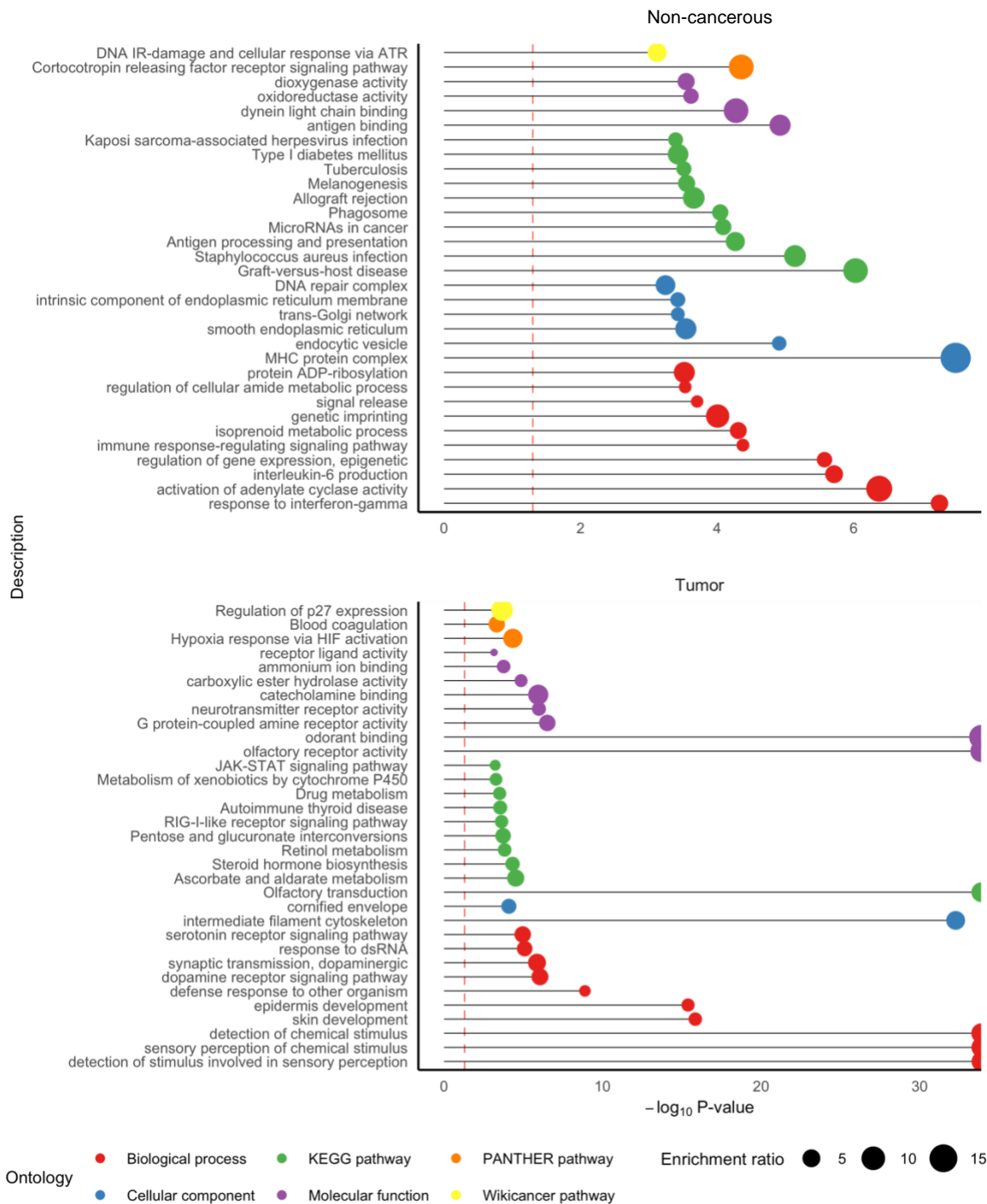


**Supplemental Figure S1: Analysis scheme.** We analyze genetic and transcriptomic data from non-cancerous breast and prostate tissue from GTEx and breast and prostate tumors from TCGA. We optimize eQTL mapping using ordinary least squares regression for numbers of genotype principal components and expression hidden covariates with prior to optimize eQTL discovery. We then conduct a genome-wide local and distal eQTL analysis using the optimized set of covariates. Next, we conduct mediation analysis or gene-based association testing to identify distal-eQTLs of pcGenes that are mediated by local-eQTLs of ncRNAs. Lastly, we integrate eQTLs results with GWAS using colocalization and analysis of genetically-regulated expression.

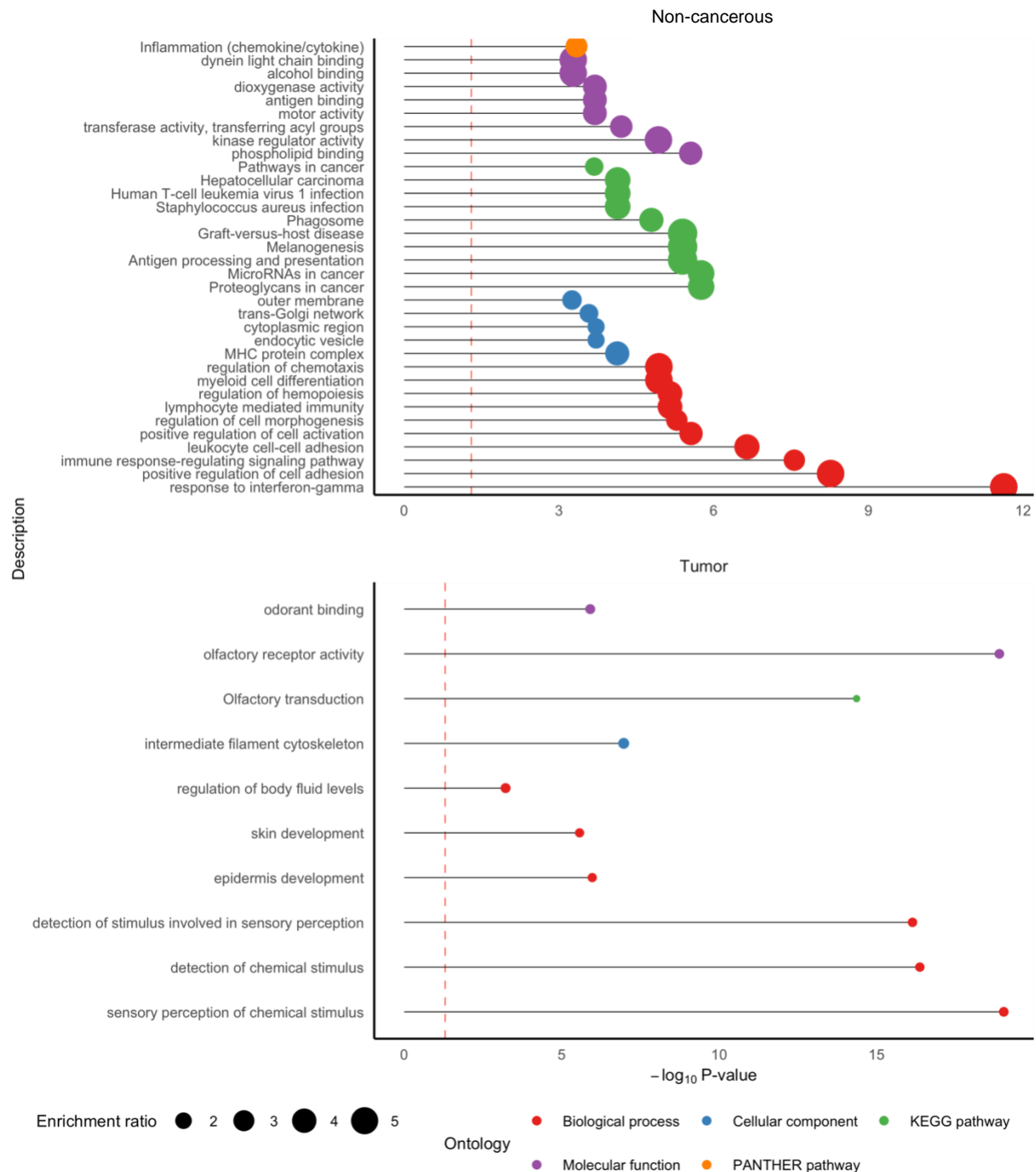




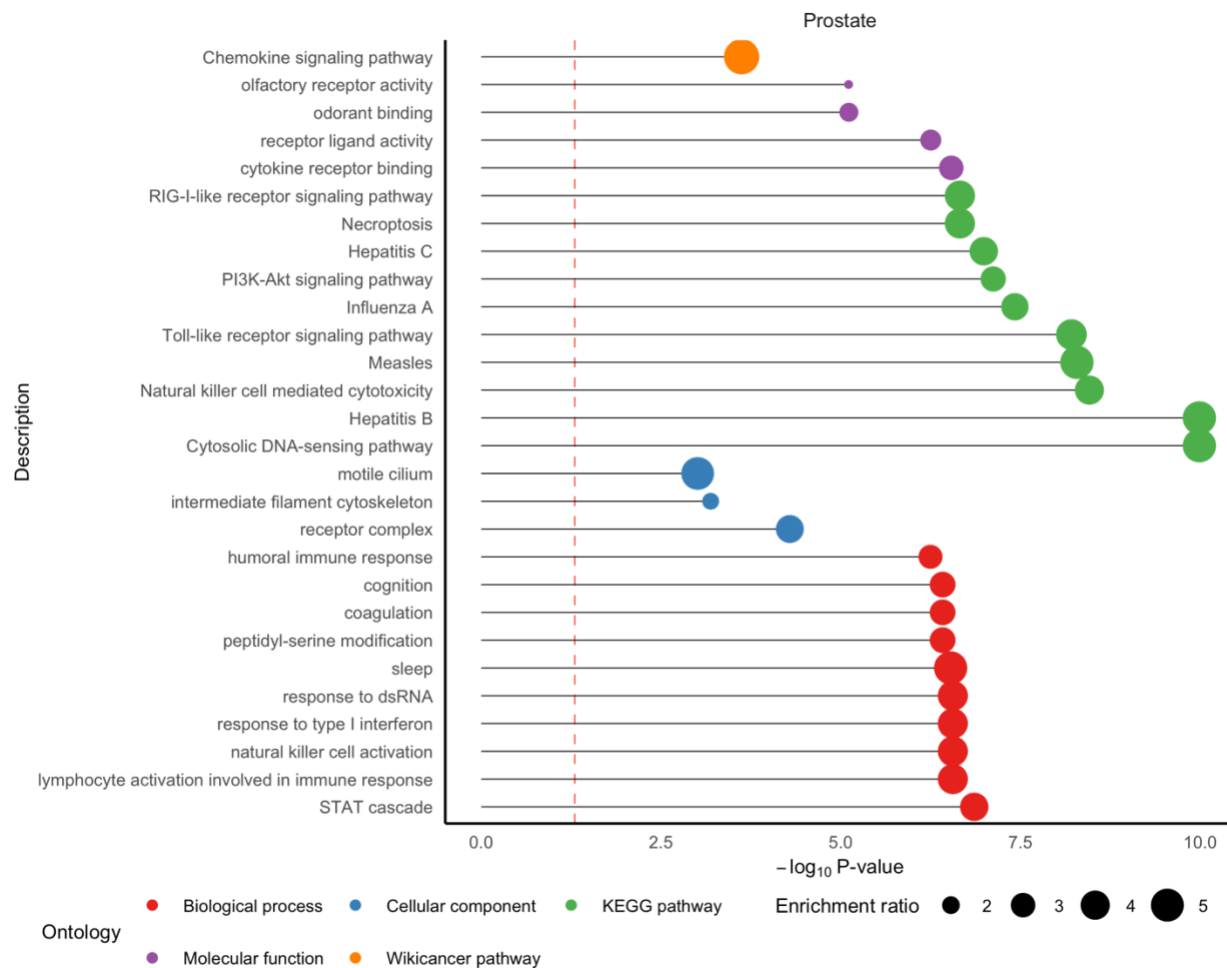
**Supplemental Figure S2:** *Distribution of total mediation effects, mediation proportions, and gene-level distal effect sizes in healthy and tumor breast and prostate tissue.*



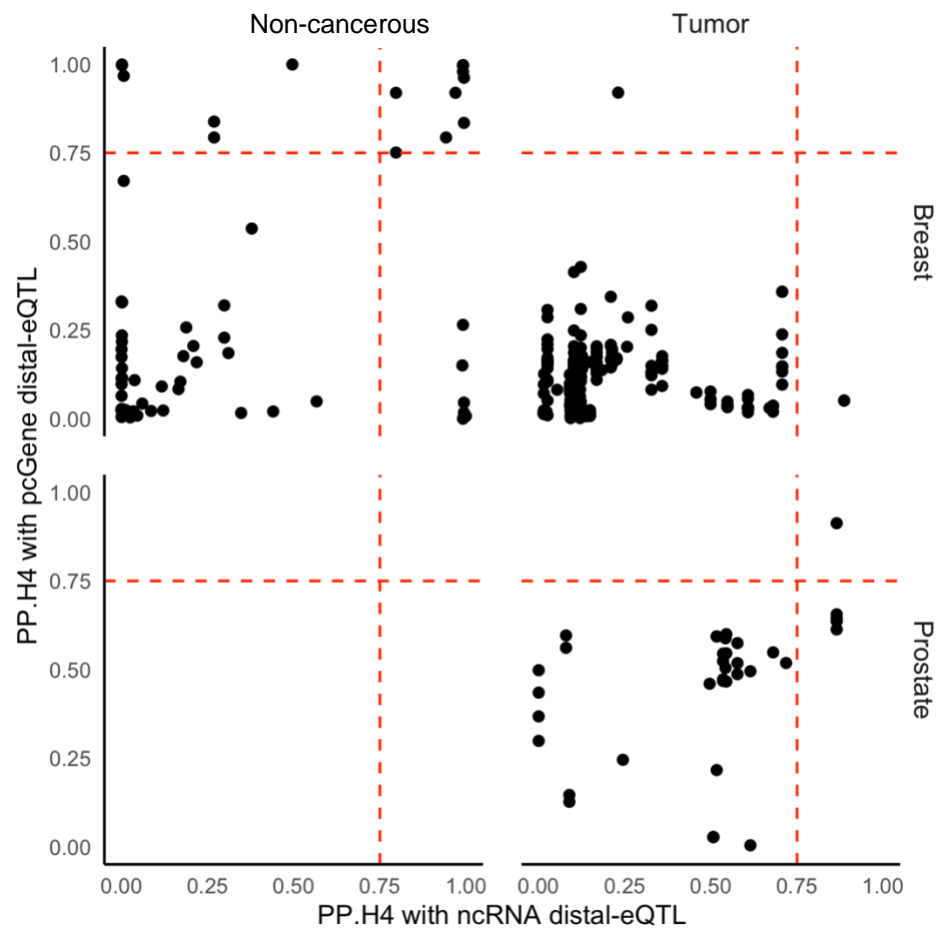
**Supplemental Figure S3:** Over-represented ontologies for healthy- or tumor-specific eGenes, compared to all protein-coding genes in the transcriptome.  $-\log_{10}$  P-value of enrichment (X-axis) of over-represented gene sets (Y-axis), with point sized by enrichment ratio and colored by ontology category. Here, combining pcGenes with a distal genetic association across breast and prostate tissue, we compare the set of pcGenes from healthy or tumor state to the universe of all pcGenes in the transcriptome.



**Supplemental Figure S4:** Over-represented ontologies for healthy or tumor state-specific eGenes, compared to all protein-coding genes detected in distal-QTL mapping.  $-\log_{10} P\text{-value}$  of enrichment (X-axis) of over-represented gene sets (Y-axis), with point sized by enrichment ratio and colored by ontology category. Here, combining pcGenes with a distal genetic association across breast and prostate tissue, we compare the set of pcGenes detected for breast or prostate and compare to the universe of all pcGenes detected across breast and prostate. No enrichments at  $P < 0.05$  were detected for breast-specific pcGenes.



**Supplemental Figure S5:** Over-represented ontologies for breast or prostate-specific eGenes, compared to all protein-coding genes detected in distal-QTL mapping.  $-\log_{10}$  P-value of enrichment (X-axis) of over-represented gene sets (Y-axis), with point sized by enrichment ratio and colored by ontology category. Here, combining pcGenes with a distal genetic association across healthy and tumor state, we compare the set of pcGenes detected for breast or prostate and compare to the universe of all pcGenes detected across breast and prostate. No enrichments at  $P < 0.05$  were detected for breast-specific pcGenes.



**Supplemental Figure S6:** Scatterplot of posterior probability of colocalization for local- and distal-eQTLs with cancer risk GWAS. Red lines show  $PP.H4 = .75$ .

## SUPPLEMENTAL TABLE LEGENDS

**Table S1:** *Prioritized ncRNA-mediated distal-eQTLs of pcGenes in healthy and tumor prostate tissue.* We provide the tissue state (healthy or tumor), SNP, ncRNA, pcGene, effect size, P-value, method of detection (mediation analysis or GBAT), and closest GWAS risk SNP and P-value.

**Table S2:** *Prioritized ncRNA-mediated distal-eQTLs of pcGenes in healthy and tumor breast tissue.* We provide the tissue state (healthy or tumor), SNP, ncRNA, pcGene, effect size, P-value, method of detection (mediation analysis or GBAT), and closest GWAS risk SNP and P-value.

**Table S3:** *In-silico validation of miRNA-pcGene pairs using TargetScan.* For miRNAs detected to mediated distal-eQTLs of pcGenes, we list miRNAs shown to target the pcGene using TargetScan.

**Table S4:** *Colocalization results for ncRNA-mediated distal-eQTLs with GWAS signal of cancer risk.* We provide the trait, tissue (breast or prostate), tissue state (healthy or tumor), ncRNA and its location, pcGene and its location, posterior probabilities of colocalization between the ncRNA and pcGene with the GWAS signal, and the colocalized SNP for each signal.

**Table S5:** *GReX analysis results for ncRNAs and cancer risk.* We provide the trait, tissue (breast or prostate), tissue state (healthy or tumor), ncRNA and its location, effect size, standard error, and Z-score of association.